

1 REVISION 1

2 Inter-Laboratory Comparison of Fission Track Confined Length and Etch Figure Measurements
3 in Apatite

4 Richard A. Ketcham¹, Andrew Carter², Anthony J. Hurford³

5 ¹Jackson School of Geosciences, The University of Texas at Austin, Austin, TX, USA

6 ²Department of Earth and Planetary Sciences, Birkbeck College, Malet Street, London, WC1E
7 7HX, UK.

8 ³Department of Earth Sciences, University College, Gower Street, London, WC1E 6BT, UK,

9 Key words: GEOCHRONOLOGY: fission-track dating, track length measurement, apatite, inter-
10 laboratory calibration, thermal history analysis

11 **Abstract**

12 Apatite fission-track length and etch figure data are powerful tools for obtaining thermal
13 history information, but both require human analysts making manual measurements, and
14 reproducibility is not assured. We report the results of an inter-laboratory study designed to
15 clarify areas of congruence and divergence for these measurements and provide a basis for
16 evaluating best practices to enhance intercompatibility of data sets. Four samples of megacrystic
17 apatite from Durango, Mexico with induced tracks, one unannealed and three thermally
18 annealed by varying amounts, were distributed internationally. In all, 55 analysts in 30
19 laboratory groups participated in the experiment. Relative mean track lengths among the
20 samples were consistent across all analysts, but measurements for each sample showed scatter
21 among labs and analysts considerably in excess of statistical expectation. Normalizing
22 measurements of annealed samples using the unannealed sample improved consistency, as did

23 normalizing for track angle using c-axis projection. Etch figure data also showed variability
24 beyond statistical expectation, and consistency was improved by normalizing. Based on these
25 data we recommend rigorous analyst training for length and etch figure measurement that
26 includes measurement of standards, and that each analyst's data on unknowns be normalized by
27 that analyst's own measurements on standards when using thermal history inverse modeling as
28 part of the interpretation process.

29 **Introduction**

30 The key to resolving detailed thermal histories using the apatite fission-track (AFT)
31 system comes from combining ages with track length data. Fission tracks form over time, and
32 earlier-formed ones will experience more of a sample's thermal history than later-formed ones.
33 This leads to characteristic patterns in horizontal confined track length distributions that can
34 provide unique information on thermal history (Gleadow et al., 1986). Even greater resolution is
35 available when length data are paired with computational tools (e.g., Gallagher, 1995; Gallagher,
36 2012; Green et al., 1989; Ketcham, 2005) to identify the range of thermal histories that are
37 consistent with both the length and age data and other geological constraints, using kinetic
38 models of fission-track annealing (Crowley et al., 1991; Ketcham et al., 2007b; Ketcham et al.,
39 1999; Laslett and Galbraith, 1996; Laslett et al., 1987).

40 The ability to use track length data correctly and confidently hinges on the fidelity of the
41 length measurements, and in particular their consistency with respect to the measurements
42 underlying models of fission-track annealing (e.g., Barbarand et al., 2003a; Carlson et al., 1999;
43 Green et al., 1986). Although the analytical procedures used in these studies can be reproduced,
44 and we understand many of the geometric sources of bias associated with track observation
45 (Galbraith, 2005 Chapter 8; Galbraith et al., 1990; Ketcham, 2003), full compatibility is not

46 assured. In particular, because confined tracks are found and measured by a human analyst using
47 a microscope, rather than some mechanical or automated procedure, reproducibility of length
48 data is an important concern.

49 The reproducibility of confined length data has been considered at both the inter-lab and
50 intra-lab level. Intra-lab studies are valuable because they enable better control of conditions
51 (such as repeating measurements of the same material using the same instrumentation), and thus
52 allow focus on variables of interest. For example Green et al. (1986) include and compare
53 measurements by two analysts of the same mounts. Barbarand et al. (2003b) gathered a series of
54 induced-track data aimed at examining various aspects of reproducibility in detail, including
55 among analysts and for single analysts over time, as well as the effects of Cf irradiation and the
56 number of measurements necessary to converge to the correct mean length. Ketcham et al.
57 (2009) obtained data for several analysts on two samples with induced and spontaneous tracks,
58 and assessed the effects of measurement variability on thermal history reconstruction and the
59 potential mediating ability of normalizing for length and angle.

60 Inter-laboratory experiments, however, provide the information necessary to assess the
61 fidelity of measurements across the community and thus the overall reliability of the technique as
62 it is applied. There has only been one previous large-scale inter-laboratory experiment for length
63 measurements (Miller et al., 1993), and its outcome was mixed, indicating general agreement but
64 scatter substantially in excess of statistical expectation. Definitive interpretation was
65 complicated, however, because the material was non-ideal, consisting of aliquots of natural
66 samples with spontaneous fission tracks, which could conceivably have been non-homogeneous.
67 Also, no information was reported about laboratory techniques, such as etching method.

68 With the help and cooperation of the international AFT community, we have performed a
69 new inter-laboratory experiment designed to gather information intended to clarify areas of
70 congruence and divergence, provide a basis for evaluating best practices to enhance
71 intercompatibility of data sets, and suggest areas that merit further study.

72 **Methodological Overview**

73 *Length revelation*

74 Fission tracks are too narrow (8-9 nm diameter in apatite; Li et al., 2010) to be observed
75 under an optical microscope, and instead are revealed by their ability to etch more easily than
76 bulk crystal. Fission-track mounts are prepared by mounting grains in epoxy, polishing to reveal
77 interior surfaces, and then etching in nitric acid (HNO₃) at some prescribed conditions of
78 strength, temperature and duration. Apatite etches anisotropically (Green and Durrani, 1977),
79 with faster etching in the direction of the crystallographic **c** axis, and in general stronger etchants
80 (higher concentration and/or temperature) are expected to increase this anisotropy compared to
81 weaker ones.

82 Fission tracks intersecting the polished surface only contain partial length information, as
83 one of their ends is missing. Confined tracks are revealed when etchant travels down a pathway
84 from the exposed surface and intersects a track in which both ends are within the solid crystal.
85 When the etchant pathway is another fission track, the confined track is referred to as a TINT
86 (track-in-track; Lal et al., 1969), while if the pathway is a fracture or cleavage it is termed a
87 TINCLE (track-in-cleavage, Bhandari et al., 1971).

88 *Length measurement*

89 Confined track lengths are measured under a microscope at high magnification, generally
90 1000x-1600x, using either a drawing tube and digitizing tablet or a camera and specialized
91 software to measure the distance between track ends. As surface etch rates vary according to
92 crystallographic orientation it is normal practice to control for etching efficiency and measure
93 tracks only on grains in which the crystallographic **c** axis is in the polished plane, as these have
94 the lowest bulk etch rate. **C**-parallel sections can be determined by their aligned etch figures
95 (Donelick et al., 2005), and track orientation with respect to the **c** axis can be determined as the
96 angle between the track and the etch figure elongation direction. Confined tracks must be close
97 to horizontal, although limited inclination has little effect; the projection of a track dipping 10°
98 with respect to the polished surface is within a factor of $\cos(10^\circ)$, or 0.985, of the true length. It
99 is also possible to measure steeper tracks if the measurement system records the 3D location of
100 the endpoints and accounts for the apatite refractive index, allowing a correction to be made,
101 although one test has found non-horizontal tracks to slightly increase the standard deviation of
102 the length distribution (Jonckheere and Ratschbacher, 2010).

103 For a fission track to be considered measurable, it must be completely etched, with
104 clearly defined ends. The revelation of a track will depend on its angle relative to the **c** axis
105 (hereafter denoted as ϕ) and the etching protocol; examples are shown in Figure 1. When a
106 strong etchant (5.0 or 5.5 M) is used, tracks are most easily observed, and more likely to be fully
107 etched, when they are in the ϕ range of approximately 30-85° (Fig. 1A,B) (Barbarand et al.,
108 2003b; Donelick et al., 1999). Tracks at lower angles (Fig. 1C, D track 1; 1E track 1) are thin for
109 their entire extent. Tracks close to perpendicular to the **c** axis ($\phi > 85^\circ$) can look wide but slightly
110 distorted (Fig. 1E, track 2) or initially wide near the intersection with the etchant pathway and
111 pinched toward the ends (Fig. 1F). The distorted shape of track 2 in Fig. 1E may result in a

112 slight error in angle determination when the line connecting the endpoints is not parallel to the
113 length. In the case of thin or pinched tracks, the ends can be indistinct, making it difficult to tell
114 whether they are fully etched or not; under-etched tracks should not be measured because they
115 may not record the full length, and instead could give a spurious signal of track shortening.
116 These etching effects, combined with the anisotropy of TINT etchant pathways, impart a
117 substantial bias upon which angular populations are measured (Galbraith et al., 1990; Ketcham,
118 2003).

119 The anisotropy in etching diminishes for a weaker etchant (e.g. <2N HNO₃), reducing
120 somewhat the dissimilarity of confined tracks at different ϕ angles. However, weaker etchants
121 require longer etching times (>40s vs. 20s), and etching duration brings up additional
122 considerations (Jonckheere et al., 2007; O'Sullivan et al., 2004). There is inevitably some time
123 delay before confined tracks start to etch, which varies depending on the strength of the etchant,
124 extent of subsurface penetration along a pathway (TINT or TINCLE) and solubility
125 (composition) of the apatite. As a result, even tracks at favorable angles can be under-etched,
126 and the variability in etching time contributes to variation in measured track lengths. For similar
127 reasons, short tracks are somewhat more likely to be fully etched than otherwise equivalent
128 longer tracks, partially counter-acting the biasing effect of longer lengths being more likely to be
129 intersected and etched than shorter ones (Laslett et al., 1982).

130 Other situations that can lead to erroneous measurements are shallow tracks that intersect
131 the polished surface (Fig. 1C,D track 2), tracks with fluid-filled and thus obscured ends (Fig.
132 1G,H) and opposite-dipping semi-track pairs that appear superficially to be single tracks. Of
133 these cases, the first two will lead to erroneously short measurements, and the third can be either
134 short or long.

135 The analyst measuring fission tracks must thus constantly keep in mind, and adhere to,
136 strict criteria for determining which confined tracks should be measured and which should be
137 bypassed. There is likely to be some variability in these criteria between analysts and lab groups,
138 which will contribute to variation. Finally, measurement by microscopy or via stored digital
139 images requires some form of calibration. Methods employed include calibrated microscope
140 scale bars (typically at 1-2 μm resolution) or SEM diffraction gratings (typically $< 0.4\text{-}0.6 \mu\text{m}$
141 resolution). Calibration should be made only for the area in which the features to be measured
142 are placed. Typically this is in the center of the field of view in order to avoid the defocused
143 peripheral regions. Systems that use digitizing tablets are also vulnerable to models that have an
144 uneven spacing of grid wires. Another potential issue when a drawing tube is employed is the
145 size of the LED spot used to demark track ends; most analysts center the spot over the ends, but
146 some use an edge of the spot to attempt to make the measurement more precise. All of these
147 aspects can contribute to systematic differences between laboratories.

148 *C-axis projection*

149 In addition to anisotropy of etching, apatite fission tracks also show annealing anisotropy,
150 with tracks parallel to the **c** axis annealing more slowly than tracks oriented along the **a** axis
151 (Donelick, 1991; Donelick et al., 1999; Green and Durrani, 1977). At low to medium amounts
152 of annealing, annealing rates vary smoothly between these two orientations, and length
153 distributions are well-represented as ellipses on a polar plot (Donelick, 1991), although in detail
154 the distribution may be slightly non-elliptical (Jonckheere et al., 2007). At high levels of
155 annealing, tracks at high ϕ angles begin to shorten much more quickly and disappear while low- ϕ
156 tracks persist, a process termed accelerated length reduction (Donelick et al., 1999).

157 As annealing progresses, annealing anisotropy leads to greatly increased dispersion in
158 lengths of tracks that have experienced identical amounts of heating, as shown in experiments in
159 which induced tracks are annealed (e.g., Green et al., 1986). To compensate for this, Donelick et
160 al. (1999) introduced **c**-axis projection, which was subsequently refined by Ketcham (2003) and
161 Ketcham et al. (2007a). **C**-axis projection is a transform that converts each (l, ϕ) measurement
162 into an estimate of what the length of a track oriented along the **c** axis that had experienced the
163 same annealing conditions would be, l_c , and the uncertainty in that estimate, σ_{l_c} . It can be more
164 generally viewed as a means of removing the dispersion caused by annealing anisotropy,
165 resulting in a more precise index of thermal input for a given track than length alone.

166 Creating a **c**-axis projection model consists of fitting ellipse radii, $l_{c,fit}$ and $l_{a,fit}$
167 corresponding to the **c**-axis and **a**-axis directions, to sets of tracks measured in a series of
168 experimental annealing runs. These data are then used to fit a four-parameter projection
169 transform (Ketcham et al., 2007a). This process generally requires dozens of experiments to
170 document all stages of annealing and overcome dispersion in the ellipse fits, and thus has only
171 been done on the two largest experimental data sets, by Carlson et al. (1999) and Barbarand et al.
172 (2003a). These studies used slightly different etchant strengths, respectively 5.5 M and 5.0M
173 HNO₃, and the difference between their respective **c**-axis projection models was attributed to
174 etchant (Ketcham et al., 2007a). The present study tests whether this assertion is correct, or
175 some other factor may be responsible for variation in observed anisotropy effects.

176 *Etch figures*

177 Etch figures, the intersections of etched tracks with the polished surface (Fig. 1D), are
178 useful for determining crystallographic orientation, as a proxy for inferring the effective
179 annealing kinetics (Burtner et al., 1994; Ketcham et al., 1999) and estimating initial (unannealed)

180 track length (Carlson et al., 1999). The principal measured parameter is the diameter of the track
181 parallel to the apatite *c* axis when it is in the polished plane (D_{par}); the *c*-axis perpendicular
182 diameter, D_{per} , is also of potential use, but is more difficult to measure reliably. The Ketcham et
183 al. (2009) experiment found reproducibility among multiple analysts measuring D_{par} on the same
184 grain mounts to be poor. Sobel and Seward (2010) studied the problem under better conditions
185 and in considerably more detail, and suggest protocols for executing and normalizing D_{par}
186 measurements.

187 **Methods**

188 Preparations for the experiment began in 2004. Mark Cloos (University of Texas at
189 Austin) provided a selection of lime-colored apatite crystals from Durango, Mexico, and three
190 were selected as containing minimal defects. Each was heated at 500°C for 24 hours to totally
191 anneal spontaneous tracks. Aliquots of each crystal were polished, etched and inspected to
192 confirm total spontaneous track removal. Each crystal was sliced into ~1 mm plates parallel to
193 the *c*-axis using a fine diamond saw. The sliced crystals were wrapped in aluminum foil and
194 irradiated at the Lucas Heights reactor (Australia) in April 2004 using nominal thermal neutron
195 fluences of 2×10^{16} ncm⁻². Each crystal was irradiated in a separate reactor run (TE68, 70 and
196 77) to keep the total mass of active material within acceptable limits. Each irradiation was
197 monitored by inclusion of a CN-5 dosimeter glass with a mica detector. Substantial radioactivity
198 was allowed to decay until early 2008.

199 In 2008, induced tracks in the samples were partially annealed and aliquots distributed to
200 participating laboratories. Apatite from irradiation TE70 was designated DUR-1, apatite from
201 irradiation TE77 was divided into two aliquots designated DUR-2 and DUR-3, and apatite from
202 irradiation TE68 was designated DUR-4. Appropriate annealing conditions were estimated

203 based on Barbarand et al. (2003a), and the furnaces, annealing rig, thermocouples and all
204 procedures were identical to those used by Barbarand et al. (2003a).

205 For sample DUR-1 annealing conditions of $288\pm 2^\circ\text{C}$ and 10 hr (plus ~3 min equilibration
206 time on loading) were chosen to produce a track-length distribution similar to exhumed
207 basement, with a mean length (l_m) of 11.5-12 μm . Measurements of a test aliquot gave an l_m of
208 $12.05\pm 0.07 \mu\text{m}$ (n=100). Sample DUR-2 was left unannealed as a control sample containing
209 full-length induced tracks. For sample DUR-3 the aim was to produce a broad track-length
210 distribution as might be found in a subsurface sample, more complex to measure but with a
211 statistically-adequate number of tracks. It was annealed at $310\pm 2^\circ\text{C}$ for 10 hr (equilibration on
212 loading took about 3.5 min), and an initial test aliquot gave an l_m of $10.20\pm 1.10 \mu\text{m}$ (n=101).
213 DUR-4 was intended to simulate a volcanic-cooling type track-length distribution. It was
214 annealed at $240\pm 2^\circ\text{C}$ for 10 hr (equilibration on loading took about 2 min), and an initial test
215 aliquot gave an l_m of $13.80\pm 0.80 \mu\text{m}$ (n=102).

216 Part of the intention behind using single apatite crystals was to attempt to overcome
217 compositional variation between different grains of a large apatite concentrate. However, sample
218 compositional heterogeneity within a single crystal could still produce variation between results.
219 To help monitor such variation, the cut plates of each apatite were broken and the relative
220 positions of each sub-piece recorded by simple letter-number co-ordinates (e.g. A1, C5 etc).
221 Where possible each lab was sent the aliquots for each apatite (DUR 1,2,3&4) taken from the
222 same relative position (A1, C5 etc.); however, this system broke down in later distributions when
223 inadequate orientated material remained.

224 Fission-track laboratories known to the authors were contacted and aliquots provided to
225 those who agreed to participate. All preparation of grain mounts and measurement was done at

226 each participating laboratory using its standard operating procedures and instrumentation. A
227 survey (Supplementary Data) was also prepared to accompany all aliquots, so that laboratories
228 could report pertinent information such as etching procedures, measurement systems, and analyst
229 experience as of the time of the measurement. Survey answers are summarized in Table 1.

230 Results were returned by email. Each data set by a single analyst for a single sample was
231 given a code (1-4)-L(1-47)-A(1-6)[-Q(1-3)], where the first number indicates the DUR sample
232 number, the second is the laboratory group, the third is the analyst at that laboratory, and the “Q”
233 designation is used as needed when the analyst measured the same sample multiple times
234 (example: 1-L13-A2-Q1 refers to sample DUR-1 analyzed by lab 13, analyst 2, first
235 measurement).

236 Summary statistics were calculated for all data submitted. The angular distribution of
237 tracks in each measurement for which angle data were reported was analyzed by fitting polar-
238 plot ellipses to provide the intercepts with crystallographic **c** and **a** axes ($l_{c,fit}$, $l_{a,fit}$), following the
239 method of Donelick (1991) and Donelick et al. (1999). In results for DUR-3 that showed
240 evidence of accelerated length reduction, the shortened tracks, generally those $<7-7.5 \mu\text{m}$ at high
241 ϕ angles, were removed for ellipse fitting; numbers ranged from 0 to 16 deleted measurements,
242 the average was 2 per experiment (or 1.7% of tracks measured), and the median was 1.

243 We also calculated $l_{c,mod}$, the mean of individually **c**-axis-projected lengths, using the two
244 models given in Ketcham et al. (2007a), which characterize the Carlson et al. (1999) and
245 Barbarand et al. (2003a) data sets; for brevity, these are respectively referred to as the C99 and
246 B03 projection models in the discussion below. Which of these two models more closely
247 represents the tendencies of a given analyst may be evaluated by the extent to which $l_{c,fit}$ and
248 $l_{c,mod}$ match, or in how they co-evolve with increasing annealing.

249 **Results**

250 In all, 30 laboratory groups participated in the experiment, with 55 analysts in total, 53 of
251 which provided analyses of all four samples.

252 To evaluate variability among aliquots, two analysts in lab 32 measured three separate
253 aliquots. Lab 32 also included a virtually untrained analyst (number 4), who received only
254 enough instruction to recognize a track and measure it, as an intentional end-member case of
255 minimal experience.

256 Some laboratory groups independently decided to conduct additional measurements to
257 capture additional information. Lab 13 re-polished and re-etched each mount three times with
258 different etching protocols to inspect etching effects. Three analysts in lab 14 measured both
259 TINT and TINCLE tracks and provided summaries for each; all results are reported, but for
260 comparing among lab groups we utilize the combined results. Lab 41 performed measurements
261 with and without ^{252}Cf irradiation (Donelick and Miller, 1990) to enhance detection of confined
262 tracks.

263 *Survey*

264 Responses to the survey are provided in Table 1. We requested for one survey to be
265 submitted per analyst, although some lab groups submitted combined surveys, and others omitted
266 some questions or neglected to submit them. Experience of users represents a full continuum
267 from 38 years of experience to novice. Among those who reported at least 1 year of experience,
268 the mean was 12.5 years.

269 Results indicate a number of areas of congruence in the community. Only one lab uses
270 oil-immersion microscopy, and almost all used the straightforward method of demarking track

271 ends directly with an LED or pointer when measuring, as opposed to previously mentioned
272 strategies aimed at compensating for non-negligible LED size. Most analysts measured only
273 TINT tracks to avoid uncertainties associated with fracture movement that could increase the
274 apparent length of tracks and to avoid additional orientation bias (since cleavage in apatite is
275 oriented at {0001} and {1010}), as well as the possibility that geologic fluids could have
276 infiltrated and pre-etched or otherwise fixed tracks at some earlier stage in their history
277 (Jonckheere and Wagner, 2000).

278 Results showed an unexpected diversity of etching protocols, however. In all 14 different
279 protocols were reported, although two of these were experiments intended to test etching effects,
280 and one was an adapted procedure intentionally analogous to that used for zircon (e.g., Yamada
281 et al., 1995). Seven employed 5.0 or 5.5 M HNO₃ at slightly different temperatures; seven used
282 other etchant strengths. The number of track lengths measured on each sample varied among labs
283 and samples, from 50 to over 200.

284 *Unannealed sample, mean length*

285 There was considerable variation among results for the unannealed sample, DUR-2. Data
286 are given in Table 2, and mean track lengths and errors are plotted against several variables in
287 Figure 2. Excluding four outliers below 15 μm , there was a spread in results of almost 1.6 μm
288 (15.25-16.84 μm). Overall, only 23 of the 65 measurements reported (35%) are within 2
289 standard errors of the overall mean (15.89 \pm 0.12 μm).

290 Experience and frequency of making measurements do not seem to be factors
291 contributing to consistency of results; the most-frequent analysts (lab 13) differed from the
292 second-most frequent (lab 14) by well over 1 μm (Fig. 2B). There is a vague trend of increasing

293 mean length versus operators' frequency of analyses and years of experience (Fig. 2B, C), but
294 overall the data are scattered in this regard.

295 Interestingly, there is no evidence of a trend in initial length versus etching protocol, and
296 in particular etchant strength (Fig. 2D). Overall the amount of variation observed using the two
297 primary etching protocols employed currently (5.0 or 5.5 M HNO₃, 20s, 21°C) spans the range
298 observed with different etchant strengths and temperatures and durations.

299 *Annealed samples, mean length*

300 Figure 3 shows the mean lengths and uncertainties reported for the annealed samples, and
301 data are provided in Tables 3-5. The degree of scatter is similar to or somewhat worse than
302 obtained for the unannealed sample: in order of increasing degree of annealing (DUR-4, DUR-1,
303 DUR-3), 16 of 62 (26%), 19 of 62 (31%), and 24 of 63 (38%) reported means were within two
304 standard errors of the respective overall means.

305 *Angular data*

306 Of 55 analysts, 42 reported angular data and 13 did not. The ellipse fits to each
307 experiment are shown in Supplemental Data Figures S1-S5. For each sample, a characteristic
308 pattern of length versus angle is observed across many laboratories and analysts. In general,
309 results repeated patterns observed in the data of Carlson et al. (1999) and Barbarand et al.
310 (2003a): generally an elliptical distribution, with the possible exception of the most-annealed
311 sample DUR-3.

312 Two selected sets of ellipse fits for the four samples are shown in Figure 4; Fig. 4A-D
313 show the results for a very experienced analyst from lab 32, and Fig. 4E-H show the
314 corresponding fits for the novice user from the same lab. The measurements by the experienced

315 analyst cluster tightly around the ellipses, while the measurements by the novice are much more
316 scattered. Most of the novice's outliers were short compared to the experienced analyst's data,
317 although some were long. The analysts also diverge in that there is little systematic anisotropy in
318 the measurements of the novice, whereas the experienced analyst shows the familiar pattern of
319 increasing anisotropy at increasing levels of annealing (e.g., Donelick, 1991; Donelick et al.,
320 1999).

321 The most-annealed sample, DUR-3, experienced conditions that put it into the first stages
322 of the "accelerated length reduction" regime (Donelick et al., 1999; Ketcham et al., 1999), in
323 which tracks at high angles to the *c*-axis begin to anneal more quickly, departing from the
324 elliptical trend. Whether these shortened tracks were measured or not was an area of particular
325 divergence. Figure 5 shows six additional examples (to go with Fig. 4C and G), in which all
326 analysts had at least 19 years of experiences. These analysts range from measuring zero (top
327 row) to a few (middle row) to several (bottom row) tracks that do not fall on the elliptical trend.
328 In some cases (e.g., labs 41, 47), different analysts observing the same mount measured very
329 different proportions of non-elliptical tracks.

330 The data also show divergence in the relative frequencies of measurement of elliptical-
331 trend high- and low- ϕ tracks. For example, some analysts measured very few high-angle ($\phi > 85^\circ$)
332 tracks (Lab 5-A1; see Fig. S1 for examples in this paragraph), and others measured very few in
333 the unannealed samples but more in the annealed samples (Lab 5-A2, 34, 41). Some measured
334 very few to zero low-angle tracks ($\phi < 30-40^\circ$) in all experiments (Lab 20, 22, 30, 32-A1, 34, 41),
335 while others measured an increasing proportion of low-angle tracks as annealing progressed (Lab
336 7, 13, 14, 26, 32-A2), and others measured them with roughly equivalent frequency in all
337 samples (Lab 5, 28).

338 *C-axis projected data*

339 Both **c**-axis projection models provided $l_{c,mod}$ values that matched the fitted ellipses fairly
340 well. The B03 model fits best, with a mean residual ($l_{c,fit} - l_{c,mod}$) of $-0.02 \mu\text{m}$ and standard
341 deviation of $0.56 \mu\text{m}$, whereas C99 model has a mean residual of $-0.30 \mu\text{m}$ and standard
342 deviation of $0.58 \mu\text{m}$. The cause of this difference is made evident (Fig. 6A) by comparing the
343 $l_{c,fit}$ vs. $l_{a,fit}$ points against the lines that define their relationship (Donelick et al., 1999, Equation
344 1) in the two projection models. The B03 line passes through the center of the data, and the C99
345 line intersects a cluster of points implying a steeper slope, or more quickly increasing anisotropy
346 with increasing annealing.

347 To further examine the data, lines were fitted to the four $l_{c,fit}$ vs. $l_{a,fit}$ data points for each
348 sample by each analyst. The resulting slope and intercept parameters are shown in Figure 6B.
349 The B03 line parameters lie in the midst of the resulting point cluster, while the C99 parameters
350 are close to the high-slope extreme, excluding outliers.

351 When deriving the two **c**-axis projection models, Ketcham et al. (2007a) postulated that
352 their difference in slope may be due to the difference in etchant strength, with stronger etchant
353 leading to higher anisotropy. This idea can be tested with the data in this study by observing
354 how slope varies with etchant across the range used in this study (Fig. 6C). Overall, we find no
355 clear signal; the range of slopes obtained for 5.0 M HNO_3 encompasses the entire range observed
356 for both 5.5 M HNO_3 and also weaker etchants. The strongest etchant (7 M HNO_3) appears to
357 feature the highest slope, but those data are among the outliers. The slopes from the lab 13
358 experiments testing various etchant strengths by the same analysts also show no clear pattern;
359 analyst 1 got equivalent slopes for the strongest and weakest etchants, and the highest slope for
360 the 5.0 M HNO_3 , while analyst 2 got the lower slope for the 5.0 M and the highest for the

361 weakest etchant. In part, these results reflect that the four-point line fits have considerable
362 variability.

363 *Replicate analyses*

364 Replicate analyses by lab 32 showed no evidence of variation among aliquots. Although
365 there was some divergence between answers beyond predicted statistical uncertainty, these were
366 not systematic. For example, analyst 1 measured the longest mean track length on the third
367 aliquot of sample DUR-2, whereas analyst 3 measured the shortest. On none of the four samples
368 did they agree on the aliquot with the longest and shortest mean length. We thus conclude that
369 variation among the apatite crystals in this study is at most a secondary effect.

370 *TINT vs. TINCLE and ^{252}Cf irradiation*

371 We detected no indication in the reported data, particularly those for lab 14, that TINT
372 and TINCLE measurements systematically diverge. Similarly, measurements obtained using
373 exclusively tracks revealed by ^{252}Cf irradiation by lab 41 analysts 2 and 5 showed no significant
374 or systematic differences from other measurements by lab 41.

375 *Normalization*

376 The large degree of variation observed among laboratories and analysts is likely to be due
377 in part to persistent factors, such as laboratory instrumentation or procedures or systematic
378 differences in analyst training or decision-making. We thus used the results for unannealed
379 samples (DUR-2) for each analyst to normalize results for their annealed samples.

380 The results of two normalizations are shown in Figure 7. Normalizing based on the mean
381 length of DUR-2 (Fig. 7A-C) considerably increases agreement among the data. The proportions
382 of analyses within 2 standard errors of the overall mean increase to 48%, 37%, and 49% for

383 DUR-4, DUR-1, and DUR-3, respectively. Convergence is similar and perhaps somewhat better
384 when the track length data are c-axis projected with the B03-based model (Fig. 7D-F), with 42%,
385 43%, and 52% of analyses within two standard errors of the mean. Though the comparison is
386 imperfect because not all analysts reported angle data, it is noteworthy that this improvement
387 comes despite the smaller uncertainties of the c-axis projected means, which feature standard
388 errors on average 29%, 33%, and 42% smaller for DUR-4, DUR-1, and DUR-3, respectively.

389 *Etch figures*

390 Figure 8 summarizes the measurements of etch figure long axis diameter (D_{par}). As with
391 the track length data, measurements for the unannealed sample show considerable variation.
392 Interestingly, as with the track length data, this variation does not seem to correlate with etching
393 procedure. If one considers the two principal protocols (5.0M and 5.5M HNO₃, 20s, 21°C), it
394 would be expected that the stronger etchant would result in larger etch figures (Sobel and
395 Seward, 2010). However, the aggregate data do not show this (Fig. 8B).

396 Again, we normalized the D_{par} data for the annealed samples for each analyst using their
397 respective measurements for sample DUR-2 (Fig. 8C). With the exception of some outliers, data
398 for a given analyst are shown to be generally consistent to within $\pm 10\%$. The slightly lower
399 normalized values for DUR-3 provide some indication that D_{par} may be influenced by annealing,
400 although the effect is subtle. The lesser degrees of D_{par} shortening in the other annealed samples
401 may be due to the less severe annealing conditions, or slight chemical variation; DUR-2 and
402 DUR-3 are from same crystal, whereas the other experiments were from different crystals.

403 **Discussion**

404 Although concerns about the reproducibility of track-length data certainly arise from
405 these experiments, the predominant picture has many positive aspects. Given that this
406 experiment was used in part as a training aid by many laboratories (for example, as a benchmark
407 for inexperienced analysts), full congruence of measurements is unrealistic. Length
408 measurements by all analysts arranged all samples into their correct ordering in term of
409 annealing level, and the fact that the angular pattern observed by Carlson et al. (1999) and
410 Barbarand et al. (2003a) is now repeated across many laboratories is an encouraging sign of
411 consistency in the community. Also encouraging is that many of the differences among analysts
412 are systematic enough that they can be substantially reduced by normalization with respect to a
413 uniform standard of unannealed induced tracks.

414 It is important to note that there is no “correct” answer, as there will always be real
415 differences due to etching, microscopy, and analyst decision-making. However, there are
416 “incorrect” answers, which can be recognized as departures from the widely-observed patterns.
417 These took a variety of forms: scatter at all angles (L05-A2, L21-A3, L25-A1, L32-A4);
418 increased observation of short tracks across various angles (L38-A1 samples 1 and 4, 1-L21-A5,
419 L28-A2, L14-A3 samples 2 and 4); scattered or short low-angle tracks (4-L21-A1); out-of-place
420 short high-angle tracks (4-L12-A1).

421 A very interesting result is how non-influential etching is to the overall patterns in these
422 data. There are no strong tendencies observed that can be traced to etching variations,
423 particularly among the most commonly-employed protocols. This indicates that most variation
424 present is due to the analyst rather than the etching procedure used. We stress, however, that we
425 are not at all diminishing the importance of strict attention to detail when etching; this study was
426 not designed to test the consequences of poor etching procedure.

427 **Recommendations**

428 The two most crucial lessons that arise from the results presented here are the importance
429 of normalization and training. Also of interest is the optimal method for c-axis projection among
430 laboratories that use it. We present below recommendations for each of these.

431 *Normalization*

432 All length measurements should be normalized before interpretation using thermal
433 history inverse modeling, to ensure that they are compatible with the measurements underlying
434 the annealing models. As a minimum step, initial length track should be normalized to Durango
435 apatite, either using sample DUR-2 from this study or an independently-created induced-track
436 sample. However, insofar as initial induced track length is known to vary with apatite chemistry
437 and solubility (Carlson et al., 1999), a more thorough procedure that takes this into account is
438 preferable. The measurable parameter that is best-correlated with initial track length is D_{par}
439 (Carlson et al., 1999). Four methods might thus be considered:

440 1) *Use the DUR-2 measurement as the “initial track length” for modeling software.*

441 This is at best a first-order correction, as it neglects that Durango apatite actually has
442 a slightly longer initial track length than typical F-apatites (Carlson et al., 1999),
443 which are the most commonly-encountered variety in practice.

444 2) *Adjust length measurements using DUR-2, and use published models for*
445 *extrapolation.* An adjustment factor for mean length, a_{lm} , based on DUR apatite can
446 be calculated for an analyst as:

$$447 \quad a_{lm} = \frac{l_{m,DUR,published}}{l_{m,DUR,analyst}} \quad (1)$$

448 where the numerator is the unannealed induced Durango mean track length

449 measurement underlying the published annealing model calibration (i.e. from Carlson
450 et al., 1999 or Barbarand et al., 2003) and the denominator is a particular analyst's
451 corresponding measurement. Length measurements can be multiplied by this factor
452 before being entered into modeling software, or the software may allow entry of a_{lm} .
453 It carries the advantage of still using etch figures or composition (assuming they are
454 measured) to better approximate initial length, and leverages the many measurements
455 that underlie the published calibrations. If etch figures are used, they would require a
456 similar adjustment factor:

$$457 \quad a_{Dpar} = \frac{D_{par,DUR,published}}{D_{par,DUR,analyst}} \quad (2)$$

458 The primary shortcoming of this solution is that it is based on a single measurement,
459 which provides only limited information on whether there is a change in how length
460 varies among apatites.

461 3) *Use the same method as 2, with more apatite varieties.* Sobel and Seward (2010)
462 advocate a cross-calibration of D_{par} data using two apatite standards, Durango and
463 Fish Canyon, in which the user-measured values are plotted against the published
464 ones, and a line is fitted through them which also passes through the origin. This
465 approach is mathematically equivalent to option 2 above, simply averaging together
466 two or even more apatites, and can be applied equally to length data. Thus:

$$467 \quad a_{lm} = \frac{\sum l_{m,published}}{\sum l_{m,analyst}} \quad (3)$$

$$468 \quad a_{Dpar} = \frac{\sum D_{par,published}}{\sum D_{par,analyst}} \quad (4)$$

469 This approach has the advantage of being less sensitive to a single analysis, and
470 incorporating information from different apatites.

471 4) *Construct complete new calibrations between initial track length and solubility or*
472 *composition using multiple apatites.* This method would be most rigorous, but also
473 the most demanding, both in terms of effort and the demands placed upon the
474 experimental material. In particular, it would be necessary to have samples spanning
475 the range of solubility/composition, as well as the variability in the initial track length
476 documented in F-apatites (Carlson et al., 1999).

477 Figure 9 illustrates normalization methods 1 through 3, using data measured by an analyst
478 for Durango and Fish Canyon standards (DUR $l_m=16.05\pm 0.08 \mu\text{m}$, $D_{par} = 1.98\pm 0.03 \mu\text{m}$; FCT
479 $l_m=16.05\pm 0.08 \mu\text{m}$, $D_{par} = 2.44\pm 0.04 \mu\text{m}$). In this example it is assumed that the analyst has
480 decided that the C99 c-axis projection model is more appropriate, and thus the measurements
481 should be normalized based on Carlson et al. (1999) data. The track length measurements are
482 systematically lower than the corresponding ones from Carlson et al. (1999), but the D_{par}
483 measurements are slightly higher (DUR $l_m=16.21\pm 0.08 \mu\text{m}$, $D_{par} = 1.83\pm 0.03 \mu\text{m}$; FCT
484 $l_m=16.38\pm 0.08 \mu\text{m}$, $D_{par} = 2.43\pm 0.04 \mu\text{m}$). Figure 9 shows the Carlson et al. (1999) l_m and D_{par}
485 data, with apatites DUR and FCT highlighted, along with the published linear fit. The analyst's
486 corresponding measurements are plotted, as well as the linear relationships based on each
487 normalization method. Method 1 provides an invariant line, which is sub-optimal but arguably
488 defensible if only near-end-member F-apatites are being considered. Method 2 captures the
489 variation in initial length documented by Carlson et al. (1999), but with a slightly different slope
490 caused by the 7.6% increase in D_{par} values ($a_{l_m} = 1.010$, $a_{D_{par}} = 0.924$). When results for FCT
491 apatites are averaged in (method 3), the slope becomes more similar to the published one due to
492 the D_{par} increase being reduced to 3.4%, which is further offset by the l_m decrease of 1.1% ($a_{l_m} =$
493 1.011 , $a_{D_{par}} = 0.966$).

494 Of the options discussed, our recommendation is that analysts use method 3, or otherwise
495 method 2 if further annealed standards with induced tracks cannot be obtained. These options
496 leverage the large amount of existing calibration data that underlie the published relationships
497 between initial length and solubility or composition, which makes them more likely to give
498 reasonable answers when applied to unusual apatite varieties (i.e. large etch figures). Although
499 the difference between methods 2 and 3 is minor in the example shown in Figure 9, we feel that,
500 analogously to age zeta calibration (Hurford, 1990), best practice requires evaluation of multiple
501 standards. The effort required for option 4 is probably only justified if the etching protocol is
502 severely changed, such as by using a weak etchant and/or substantially longer etching times.

503 A full analysis of the ramifications of neglecting normalization for inverse modeling are
504 beyond the scope of this study, as they are very context-dependent based on the types of samples
505 and geological histories being investigated. Ketcham et al. (2009) showed that omitting
506 normalization affected the shape of the fitted cooling path and the final cooling temperature in
507 cooling-only histories, and the maximum reheating temperature in non-monotonic histories.

508 *C-axis projection*

509 C-axis projection seems to increase inter-laboratory compatibility, and accounts for some
510 differing operator tendencies, particularly at strong levels of annealing. It also removes a
511 substantial component of noise: all tracks at a given level of annealing (i.e. Fig. 5) reflect the
512 same thermal input despite their difference in length, and c-axis projection responds by utilizing,
513 rather than discarding, the information in track angle.

514 It is worth reconsidering which is the appropriate c-axis projection model for a given
515 analyst or lab group to use. The B03 model seems to represent the majority of the community,
516 but some labs are better represented by C99 model. The spread in Figure 6B indicates that four-

517 point fits are not enough data to make a definitive judgment in any single case, however. The
518 C99 model tends to result in larger $l_{c,mod}$ values, because increased anisotropy means that the
519 lengths of high- ϕ tracks are increased more when being projected to **c**-axis-parallel. Thus, in
520 Figure 7D-F, the C99 projection model will cause the data for a given lab or analyst to move
521 rightwards, slightly at low degrees of annealing and more at higher degrees. In some cases this
522 step can increase compatibility among analysts and lab groups; for example, using C99 for lab 13
523 appears on the whole to increase intercompatibility with other large lab groups (14, 32).

524 It is in fact possible to create a “tunable” parameter that adjusts the projection model
525 slope+intercept to maximize compatibility among laboratories. However, we are cautious about
526 recommending such a step, as we have not ascertained the reasons underlying this apparent
527 change in the evolution of anisotropy among analysts. The divergent answers in C99 and B03
528 are both real, as they each reflect dozens of careful experiments, but we don’t yet know what
529 makes them real. Also, again, some divergences observed in this study are likely to be simply a
530 case of inadequate training or attention to detail, and it would be unwise to create a fudge factor
531 to compensate for this rather than addressing the root of the problem.

532 We thus recommend that each lab evaluate for itself which is the preferable model to
533 employ, using the four samples from this study, or equivalents, to decide which more closely
534 reflects the measurements they produce. The model chosen should be reported when thermal
535 history inversion is used.

536 *Training*

537 In addition to the protocols developed by experienced workers for their respective
538 laboratories, the samples distributed in this study can be a useful training resource. In particular,
539 we recommend a training regimen of measuring these four samples (or equivalents) and

540 critiquing the results, if necessary repeatedly, until they are judged suitably compatible with the
541 community, before measurement and utilization of track lengths for research is undertaken.
542 Results should be evaluated not only for the usual mean and standard deviation but also for
543 consistent distribution with angle, and careful attention to how borderline cases are evaluated and
544 pitfalls avoided.

545 These mounts are good for training and inter-laboratory comparison, but not perfect.
546 They are simple length-angle distributions, and after an analyst begins to measure a pattern may
547 be recognized, which can in turn bias further measurements of that sample. Measuring “blind”
548 (i.e. not seeing tables or summaries of measurements as they are made) is thus crucial. The use of
549 megacryst slabs does not test for grain selection, and the plentitude of tracks may shift an
550 analyst’s bias in evaluating track suitability (i.e. borderline cases may be more likely to be
551 passed over). Measurement of the samples in this study also provides no information about
552 relative probability of sampling from different length populations, and whether this tendency
553 varies among analysts. In view of these considerations, samples containing multiple, known
554 annealed populations would be a valuable additional inter-calibration and training tool, and are
555 being created by the lead author.

556 **Implications**

557 The results of this study indicate that there has been some degree of scatter in apatite
558 fission-track length data used for research that can be traced to the human element in their
559 measurement, which in turn is likely to affect some aspects of thermal history inverse modeling.
560 It is also clear that a large component of the problem can be addressed fairly simply and easily
561 through normalizing for length and angle and, where necessary, enhancing training regimens.

562 The time is approaching when automated systems may take over the measurement of
563 length data, which may enhance or even come close to assuring inter-laboratory consistency.
564 Even over the interval between when most of the measurements in this study were made and the
565 present, there has been considerable progress in using image-analysis-based methods to improve
566 the picking of track end-points (Donelick et al., 2013; Gleadow and Seiler, 2013). However, full
567 automation of track identification and evaluation is still some time away, with universal
568 acceptance and adoption of these solutions even further in the future. In the intervening time, the
569 measures advocated here should serve to improve the overall quality of length data produced by
570 the fission-track community, and in turn the interpretations generated from those data.

571 **Acknowledgements**

572 Our foremost and deepest thanks go to the many individuals who participated in this
573 study. Constructive reviews by R. Flowers and K. Gallagher improved the manuscript. We also
574 thank the Jackson School of Geosciences for its support of the University of Texas fission-track
575 laboratory, and M. Tamer for helping draft figure 1 and contributing suggestions and additional
576 measurements.

577 **References**

578

579

580

- 581 Barbarand, J., Carter, A., Wood, I., and Hurford, A.J. (2003a) Compositional and structural control of
582 fission-track annealing in apatite. *Chemical Geology*, 198, 107-137.
583 Barbarand, J., Hurford, A.J., and Carter, A. (2003b) Variation in apatite fission-track length measurement:
584 implications for thermal history modelling. *Chemical Geology (Isotope Geoscience Section)*,
585 198, 77-106.

- 586 Bhandari, N., Bhat, S.G., Lal, D., Rajagopalan, G., Tamhane, A.S., and Venkatavaradan, V.S. (1971) Fission
587 fragment tracks in apatite: recordable track lengths. *Earth and Planetary Science Letters*, 13,
588 191-199.
- 589 Burtner, R.L., Nigrini, A., and Donelick, R.A. (1994) Thermochronology of lower Cretaceous source rocks
590 in the Idaho-Wyoming thrust belt. *American Association of Petroleum Geologists Bulletin*,
591 78(10), 1613-1636.
- 592 Carlson, W.D., Donelick, R.A., and Ketcham, R.A. (1999) Variability of apatite fission-track annealing
593 kinetics I: Experimental results. *American Mineralogist*, 84, 1213-1223.
- 594 Crowley, K.D., Cameron, M., and Schaefer, R.L. (1991) Experimental studies of annealing etched fission
595 tracks in fluorapatite. *Geochimica et Cosmochimica Acta*, 55, 1449-1465.
- 596 Donelick, R.A. (1991) Crystallographic orientation dependence of mean etchable fission track length in
597 apatite: An empirical model and experimental observations. *American Mineralogist*, 76, 83-91.
- 598 Donelick, R.A., Donelick, M.B., O'Sullivan, P.B., McMillan, J., Hourigan, J.K., and Juel, E. (2013) Three-
599 dimensional spatial characteristics and contents of zircon crystals from high resolution optical
600 imagery for the fission track, (U-Th-Sm)/He, and U-Th-Pb systems. American Geophysical Union
601 Fall Meeting, p. T42C-06, San Francisco.
- 602 Donelick, R.A., Ketcham, R.A., and Carlson, W.D. (1999) Variability of apatite fission-track annealing
603 kinetics II: Crystallographic orientation effects. *American Mineralogist*, 84, 1224-1234.
- 604 Donelick, R.A., and Miller, D.A. (1990) Enhanced TINT fission track densities in low spontaneous track
605 density apatites using ^{252}Cf -derived fission fragment tracks: A model and experimental
606 observations. *International journal of radiation applications and instrumentation. Part D*,
607 *Nuclear tracks and radiation measurements*, 18(3), 301-307.
- 608 Donelick, R.A., O'Sullivan, P.B., and Ketcham, R.A. (2005) Apatite fission-track analysis. In P.W. Reiners,
609 and T.A. Ehlers, Eds. *Reviews in Mineralogy and Geochemistry*, 58, p. 49-94.
- 610 Galbraith, R.F. (2005) *Statistics for Fission Track Analysis*. 219 p. Chapman and Hall, Boca Raton.
- 611 Galbraith, R.F., Laslett, G.M., Green, P.F., and Duddy, I.R. (1990) Apatite fission track analysis: geological
612 thermal history analysis based on a three-dimensional random process of linear radiation
613 damage. *Philosophical Transactions of the Royal Society of London A*, 332, 419-438.
- 614 Gallagher, K. (1995) Evolving temperature histories from apatite fission-track data. *Earth and Planetary
615 Science Letters*, 136, 421-435.
- 616 Gallagher, K. (2012) Transdimensional inverse thermal history modeling for quantitative
617 thermochronology. *Journal of Geophysical Research*, 117, B02408.
- 618 Gleadow, A.J.W., Duddy, I.R., Green, P.F., and Lovering, J.F. (1986) Confined fission track lengths in
619 apatite: a diagnostic tool for thermal history analysis. *Contributions to Mineralogy and
620 Petrology*, 94, 405-415.
- 621 Gleadow, A.J.W., and Seiler, C. (2013) Fission track length distributions in multi-system
622 thermochronology. American Geophysical Union Fall Meeting, p. T42C-08, San Francisco.
- 623 Green, P.F., Duddy, I.R., Gleadow, A.J.W., Tingate, P.R., and Laslett, G.M. (1986) Thermal annealing of
624 fission tracks in apatite 1. A qualitative description. *Chemical Geology (Isotope Geoscience
625 Section)*, 59, 237-253.
- 626 Green, P.F., Duddy, I.R., Laslett, G.M., Hegarty, K.A., Gleadow, A.J.W., and Lovering, J.F. (1989) Thermal
627 annealing of fission tracks in apatite 4. Quantitative modeling techniques and extension to
628 geological time scales. *Chemical Geology (Isotope Geoscience Section)*, 79, 155-182.
- 629 Green, P.F., and Durrani, S.A. (1977) Annealing studies of tracks in crystals. *Nuclear Track Detection*,
630 1(1), 33-39.
- 631 Hurford, A.J. (1990) Standardization of fission track dating calibration: Recommendation by the Fission
632 Track Working Group of the I.U.G.S. Subcommittee on Geochronology. *Chemical Geology
633 (Isotope Geoscience Section)*, 80, 171-178.

- 634 Jonckheere, R., Enkelmann, E., Min, M., Trautmann, C., and Ratschbacher, L. (2007) Confined fission
635 tracks in ion-irradiated and step-etched prismatic sections of Durango apatite. *Chemical*
636 *Geology*, 242, 202-217.
- 637 Jonckheere, R., and Ratschbacher, L. (2010) On measurements of non-horizontal confined fission tracks.
638 In R.W. Brown, Ed. 12th International Conference on thermochronometry, p. 60, Glasgow.
- 639 Jonckheere, R., and Wagner, G.A. (2000) On the occurrence of anomalous fission tracks in apatite and
640 titanite. *American Mineralogist*, 85, 1744-1753.
- 641 Ketcham, R.A. (2003) Observations on the relationship between crystallographic orientation and biasing
642 in apatite fission-track measurements. *American Mineralogist*, 88, 817-829.
- 643 Ketcham, R.A. (2005) Forward and inverse modeling of low-temperature thermochronometry data. In
644 P.W. Reiners, and T.A. Ehlers, Eds. *Reviews in Mineralogy and Geochemistry*, 58, p. 275-314.
- 645 Ketcham, R.A., Carter, A.C., Donelick, R.A., Barbarand, J., and Hurford, A.J. (2007a) Improved
646 measurement of fission-track annealing in apatite using c-axis projection. *American*
647 *Mineralogist*, 92, 789-798.
- 648 Ketcham, R.A., Carter, A.C., Donelick, R.A., Barbarand, J., and Hurford, A.J. (2007b) Improved modeling
649 of fission-track annealing in apatite. *American Mineralogist*, 92, 799-810.
- 650 Ketcham, R.A., Donelick, R.A., Balestrieri, M.L., and Zattin, M. (2009) Reproducibility of apatite fission-
651 track length data and thermal history reconstruction. *Earth and Planetary Science Letters*, 284,
652 504-515.
- 653 Ketcham, R.A., Donelick, R.A., and Carlson, W.D. (1999) Variability of apatite fission-track annealing
654 kinetics III: Extrapolation to geological time scales. *American Mineralogist*, 84, 1235-1255.
- 655 Lal, D., Rajan, R.S., and Tamhane, A.S. (1969) Chemical composition of nuclei of Z>22 in cosmic rays
656 using meteoric minerals as detectors. *Nature*, 221, 33-37.
- 657 Laslett, G.M., and Galbraith, R.F. (1996) Statistical modelling of thermal annealing of fission tracks in
658 apatite. *Geochimica et Cosmochimica Acta*, 60, 5117-5131.
- 659 Laslett, G.M., Green, P.F., Duddy, I.R., and Gleadow, A.J.W. (1987) Thermal annealing of fission tracks in
660 apatite 2. A quantitative analysis. *Chemical Geology (Isotope Geoscience Section)*, 65, 1-13.
- 661 Laslett, G.M., Kendall, W.S., Gleadow, A.J.W., and Duddy, I.R. (1982) Bias in measurement of fission-
662 track length distributions. *Nuclear Tracks and Radiation Measurements*, 6(2/3), 79-85.
- 663 Li, N., Wang, L., Sun, K., Lang, M., Trautmann, C., and Ewing, R.C. (2010) Porous fission fragment tracks in
664 fluorapatite. *Physical Review B*, 82, 144109.
- 665 Miller, D.S., Crowley, K.D., Dokka, R.K., Galbraith, R.F., Kowallis, B.J., and Naeser, C.W. (1993) Results of
666 interlaboratory comparison of fission track ages for 1992 Fission Track Workshop. *Nuclear*
667 *Tracks and Radiation Measurements*, 21(4), 565-573.
- 668 O'Sullivan, P.B., Donelick, R.A., and Ketcham, R.A. (2004) Etching conditions and fitting ellipses: what
669 constitutes a proper apatite fission-track annealing calibration measurement? In P. Andriessen,
670 Ed. 10th International Conference on Fission Track Dating and Thermochronology, p. Abstract
671 code DV-10-O, Amsterdam.
- 672 Sobel, E.R., and Seward, D. (2010) Influence of etching conditions on apatite fission-track etch pit
673 diameter. *Chemical Geology*, 271, 59-69.
- 674 Yamada, R., Tagami, T., and Nishimura, S. (1995) Confined fission-track length measurement of zircon:
675 assessment of factors affecting the paleotemperature estimate. *Chemical Geology (Isotope*
676 *Geoscience Section)*, 119, 293-306.

677

678

1 Figure Captions

2

3 Figure 1. Photomicrographs of confined fission tracks. Black scale bars are 10 μm , and apatite **c**
4 axis orientations marked with white arrows. (A) Transmitted light image of measurable track at
5 intermediate angle to **c** axis. (B) Reflected light image of track in A. (C) Transmitted light
6 image of tracks at $\sim 25^\circ$ to **c** axis; track 1 is measurable, but track 2 intersects surface. (D)
7 Reflected light image of field of view in C, also showing elongated etch figures indicating **c** axis
8 direction. (E) Reflected light image with track 1 near parallel to **c** axis and track 2 near
9 perpendicular. (F) Reflected light image with **c**-axis-perpendicular track with pinched ends. .
10 Images in (A-F) all obtained with transmitted light. (G) Reflected light image of track that
11 appears shortened due to fluid. (H) Same track after fluid has been removed with acetone wash.

12 Figure 2. Mean track lengths and errors (1 SE) for unannealed sample DUR-2 versus: (A) lab
13 code; (B) years since being trained in fission-track analysis as of the time study measurements
14 were made; (C) approximate number of fission-track mounts measured per year over the
15 previous 3 years; (D) etching method.

16 Figure 3. Mean track lengths and errors (1 SE) for annealed samples.

17 Figure 4. Polar plots of fission-track length measurements of four study samples from an
18 experienced analyst (A-D) and a novice (E-H). Codes refer to sample number (i.e. 1-4 indicates
19 DUR-1 through DUR-4), lab number, and analyst number.

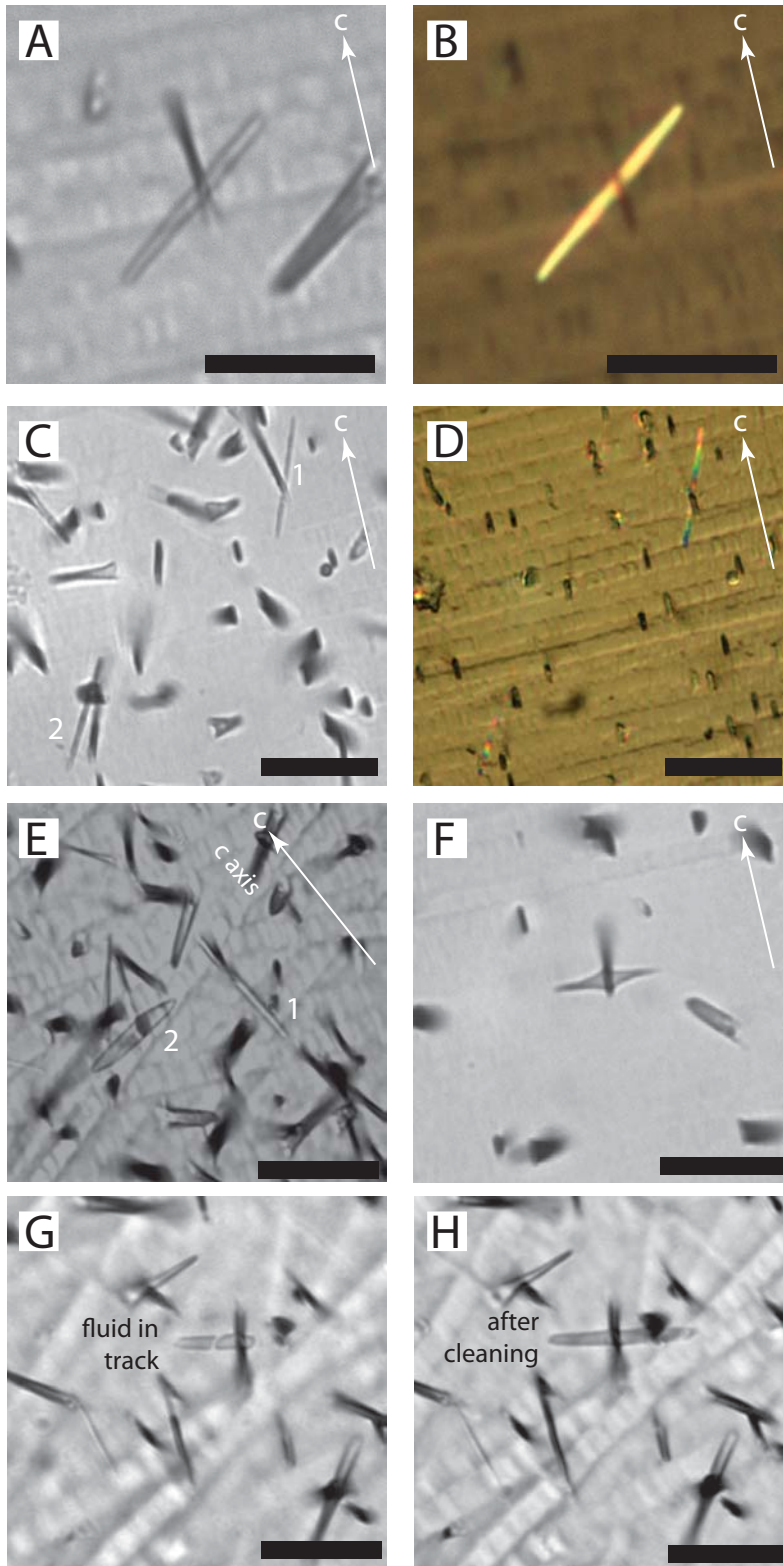
20 Figure 5. Polar plots of data for six experienced analysts for aliquots of sample DUR-3, showing
21 different tendencies for measuring shortened tracks at high angles to the **c** axis.

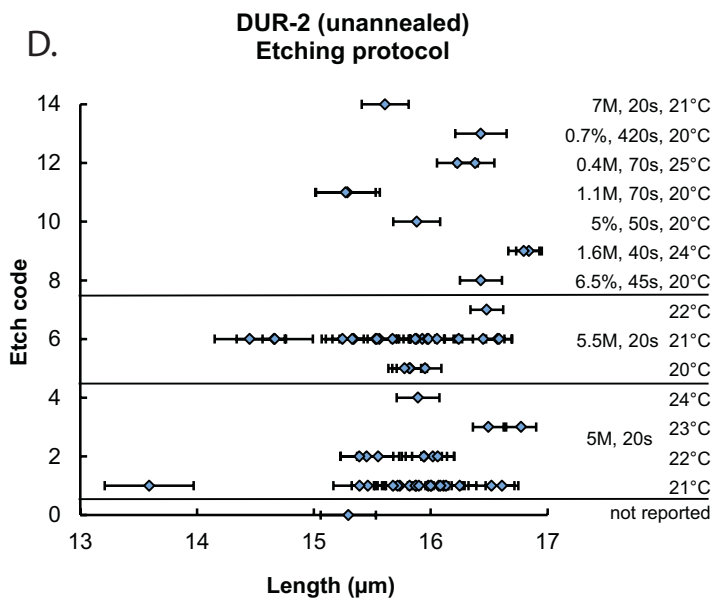
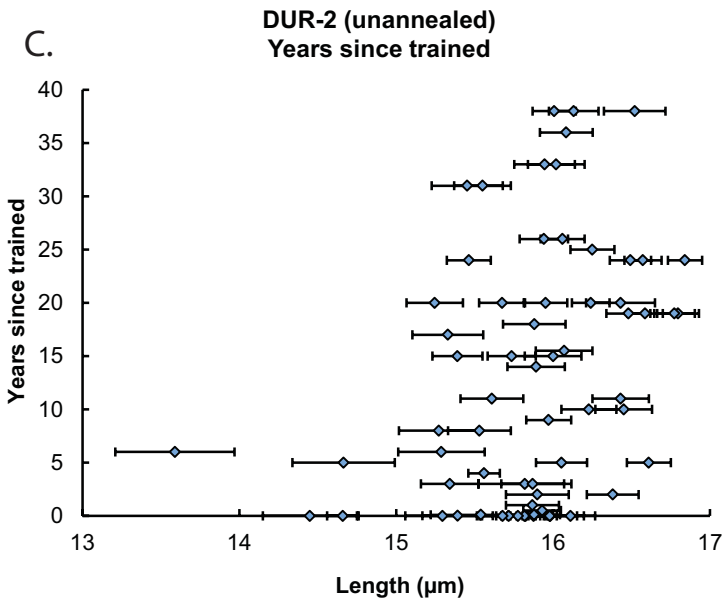
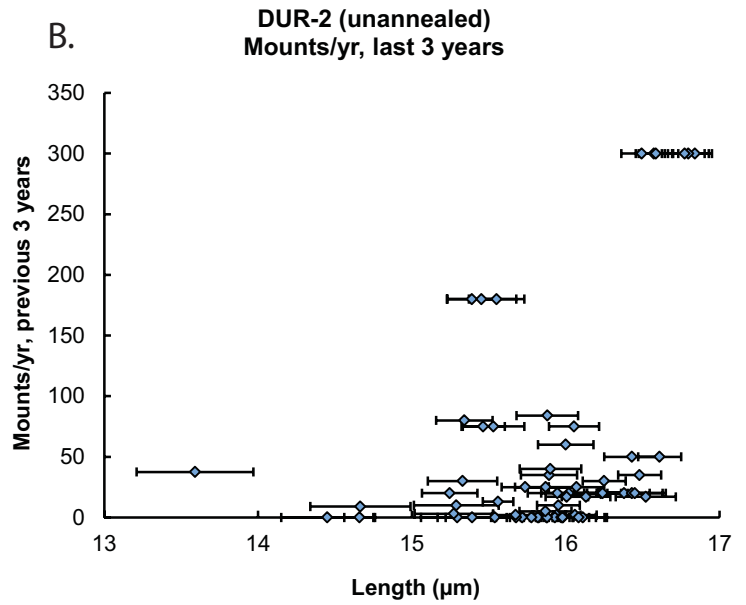
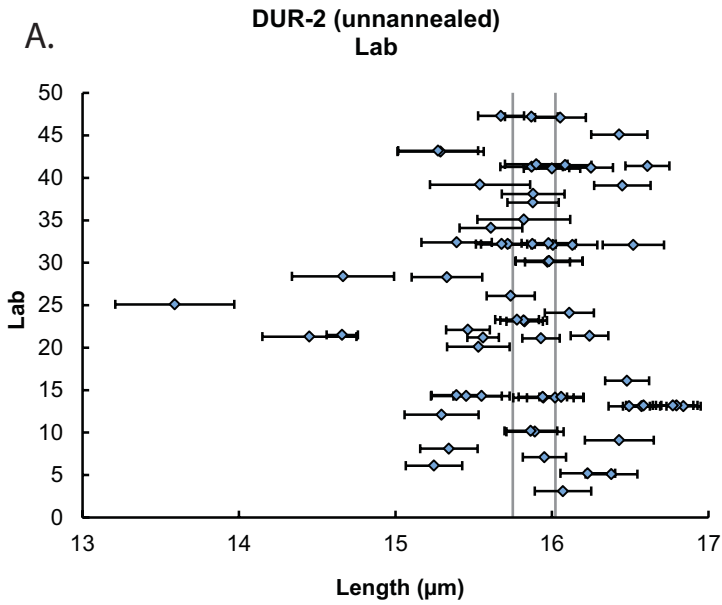
22 Figure 6. Summary plots showing evolution of track length anisotropy. (A) Individual $l_{c,fit}$ vs.
23 $l_{a,fit}$ data, with lines representing this relationship from Ketcham et al. (2007a) based on data
24 from Carlson et al. (1999) and Barbarand et al. (2003) (C99 and B03, respectively). (B) Slope
25 and intercept of lines fit to four samples for each study participant, and corresponding points
26 from C99 and B03. (C) Range of fitted $l_{c,fit}$ vs. $l_{a,fit}$ slopes for each etching method reported.

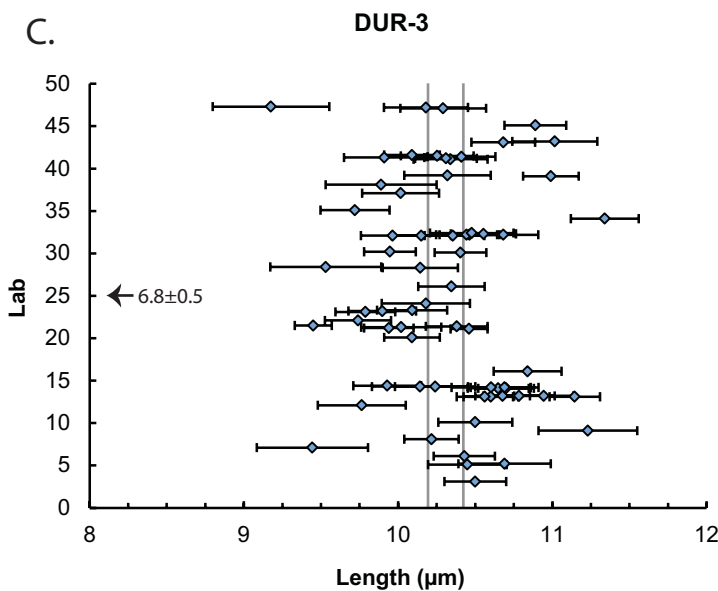
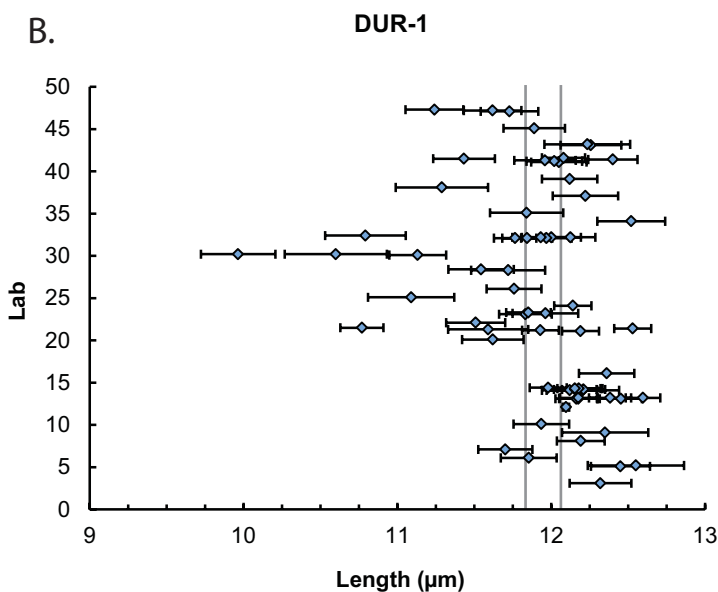
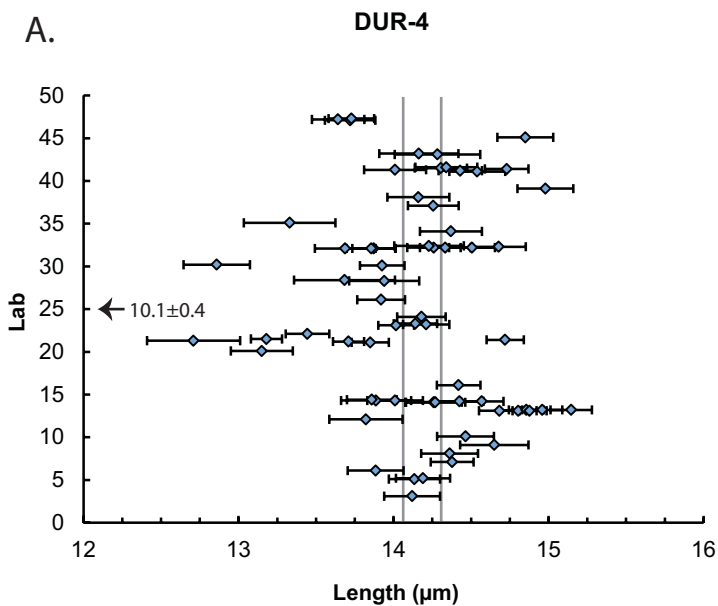
27 Figure 7. Normalized lengths and errors (1 SE) for annealed samples, for mean (A-C) and **c**-axis-
28 projected (D-F) data.

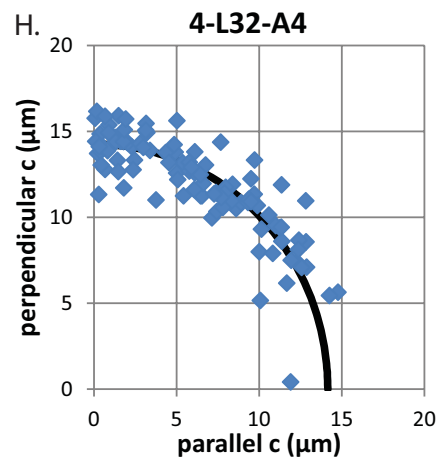
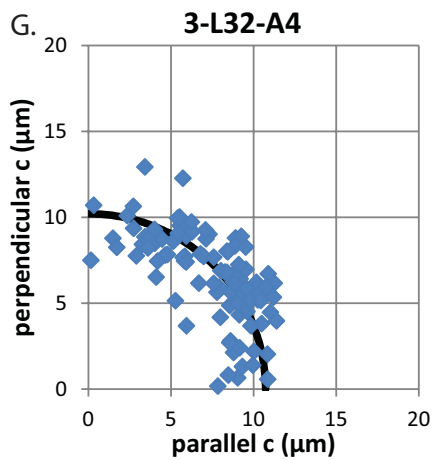
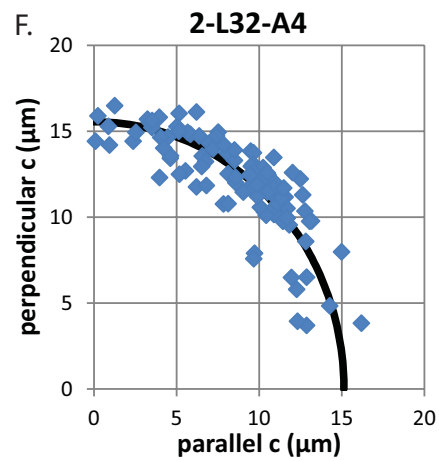
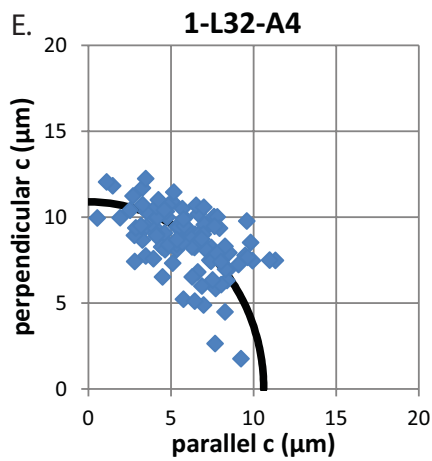
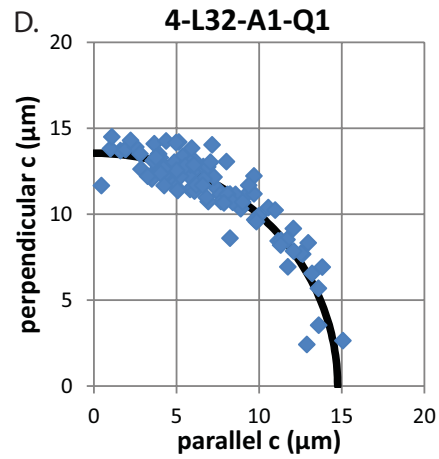
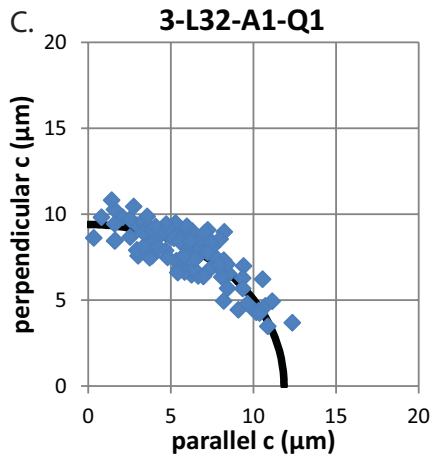
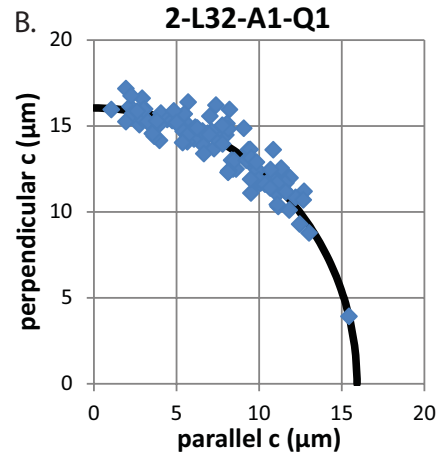
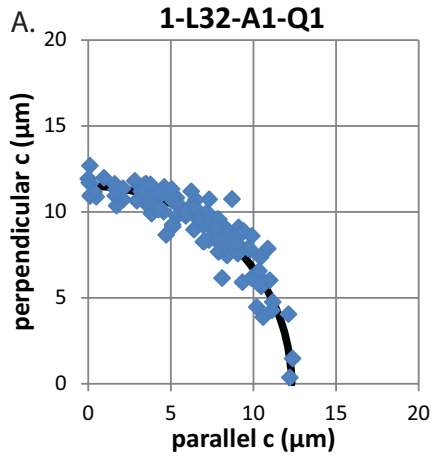
29 Figure 8. Summary plots of etch figure length (D_{par}) data. (A) Mean D_{par} and error (1 SE) versus
30 lab number. (B) Mean D_{par} and error versus etching method. (C) Normalized D_{par} values for
31 each sample.

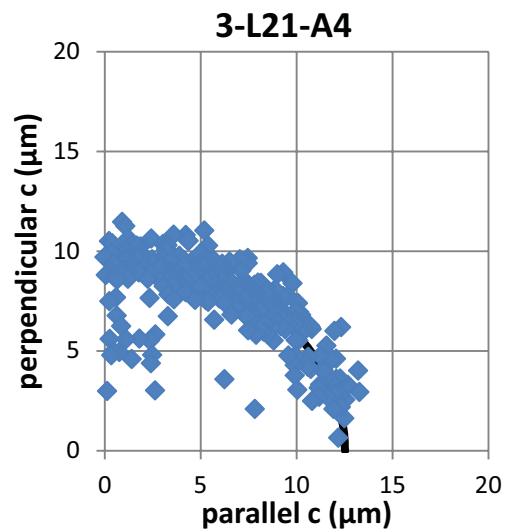
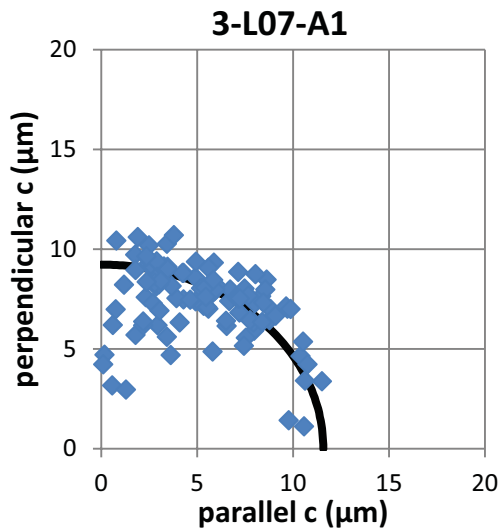
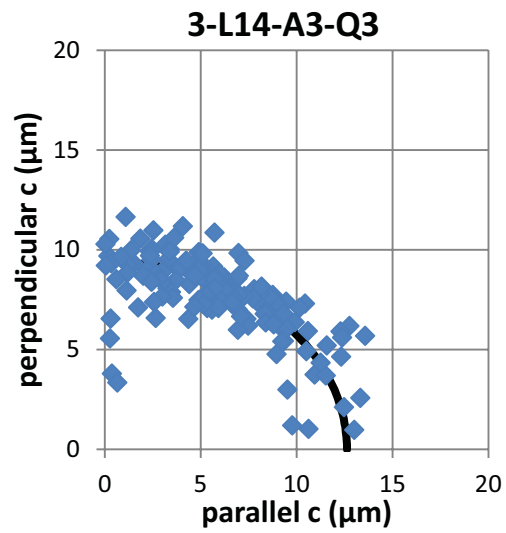
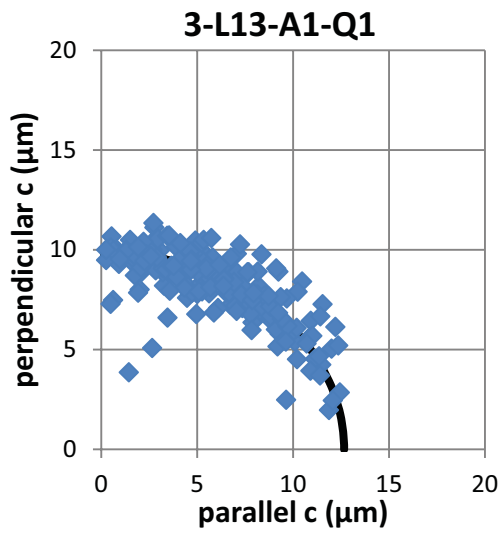
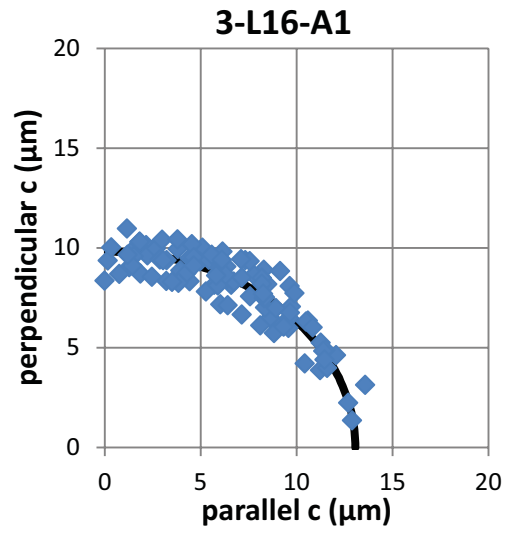
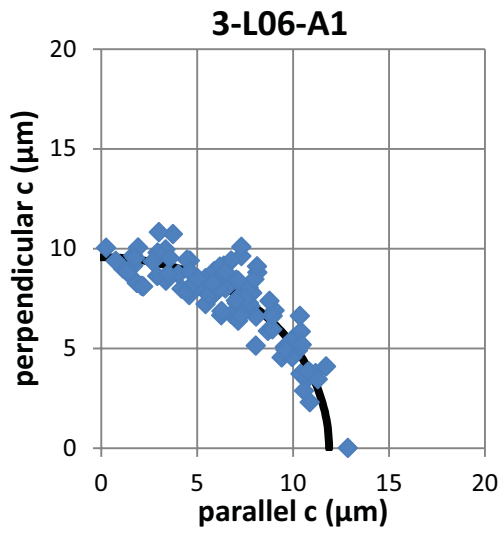
32 Figure 9. Example showing outcome of three normalization methods for track length and etch
33 figure data discussed in text.

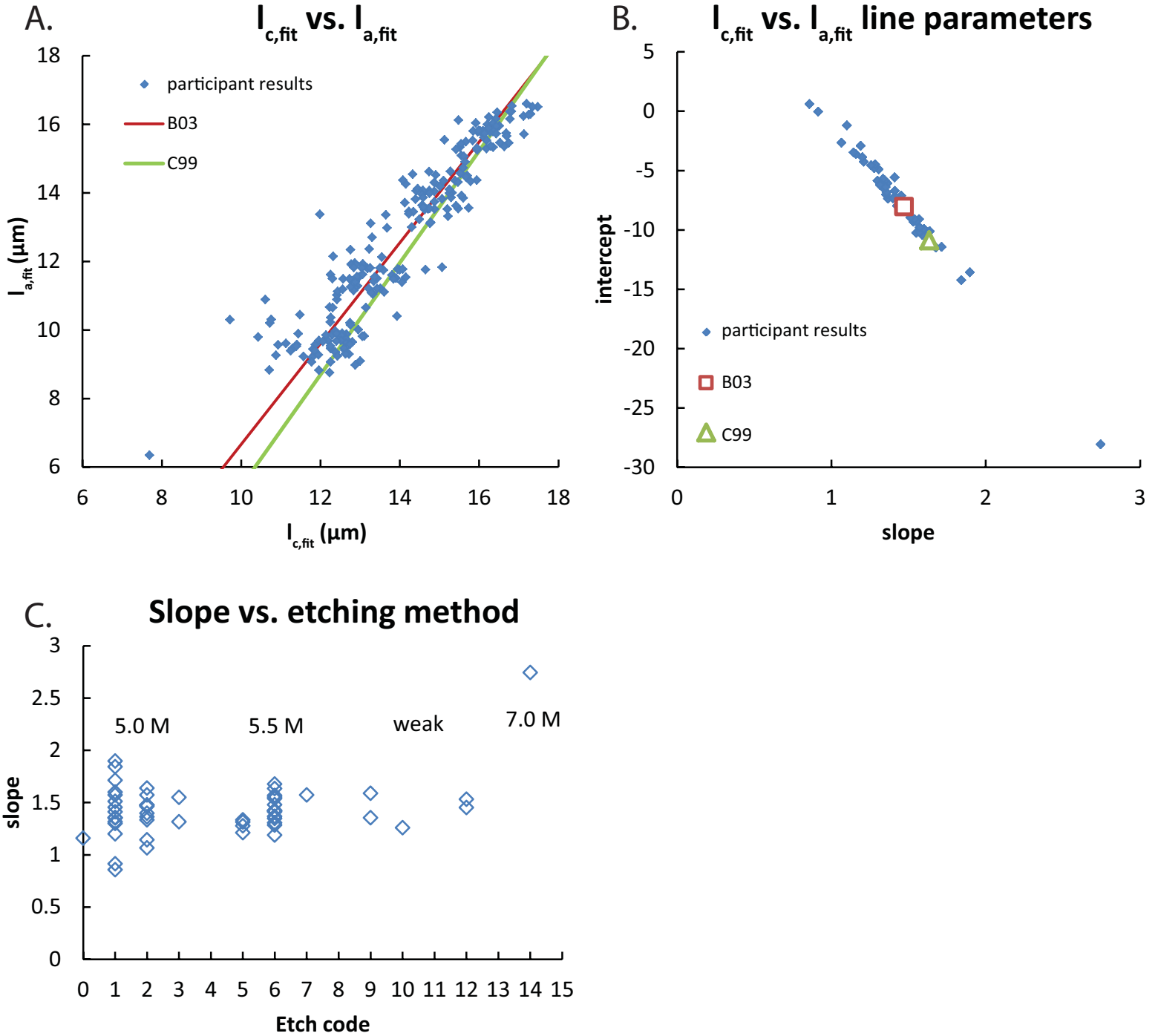


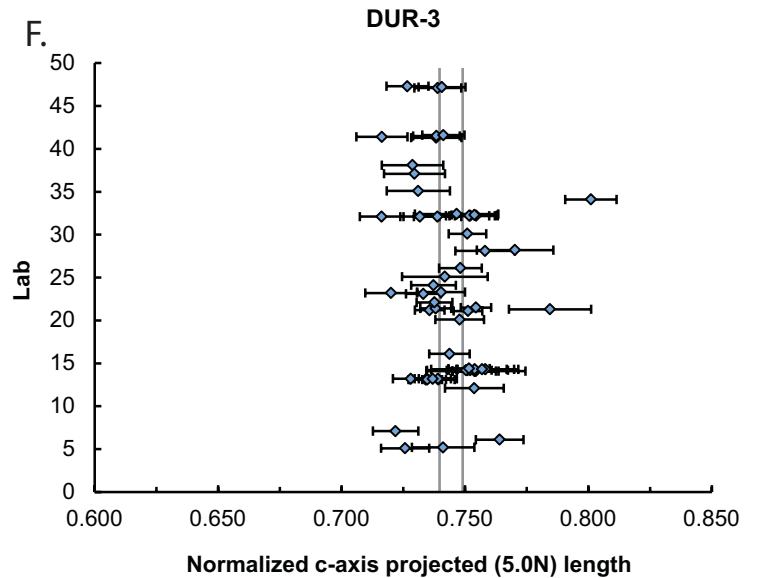
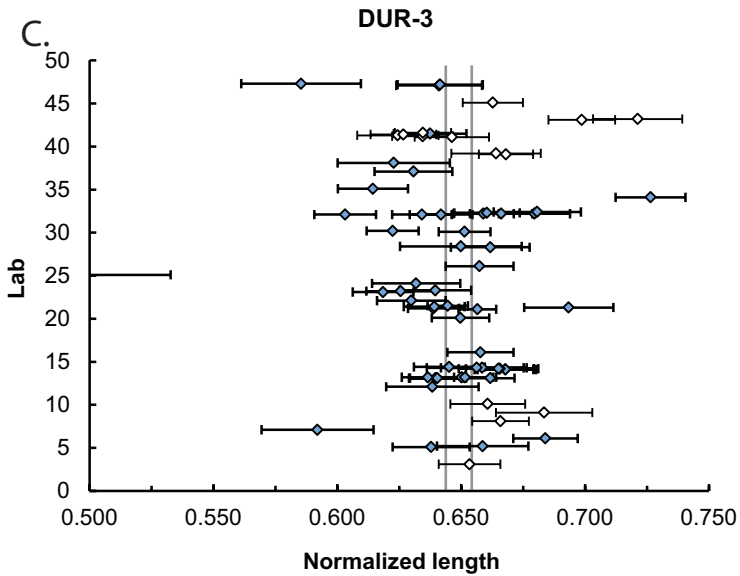
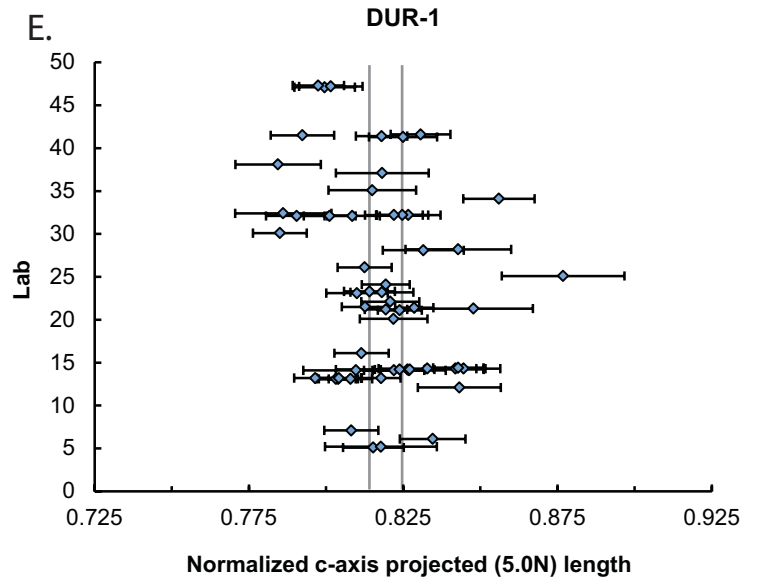
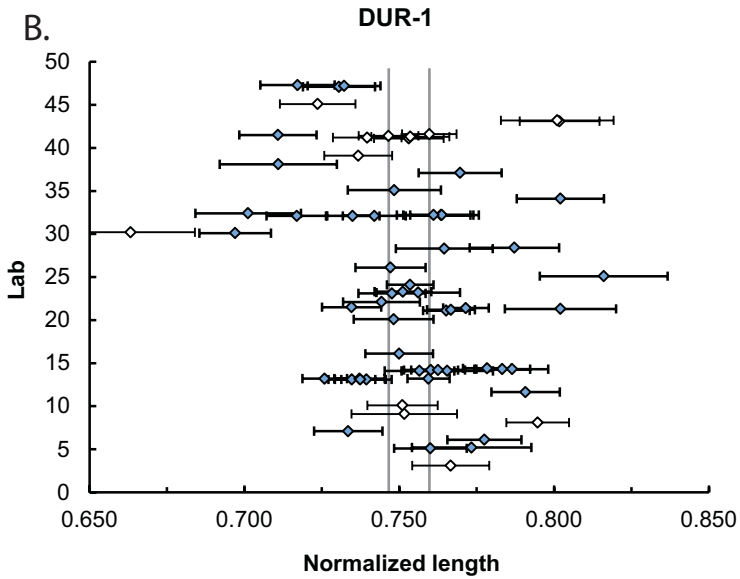
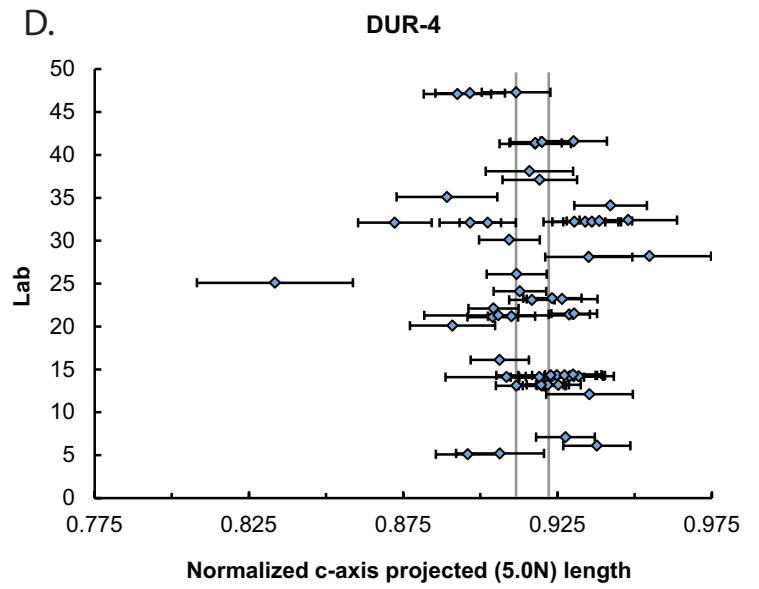
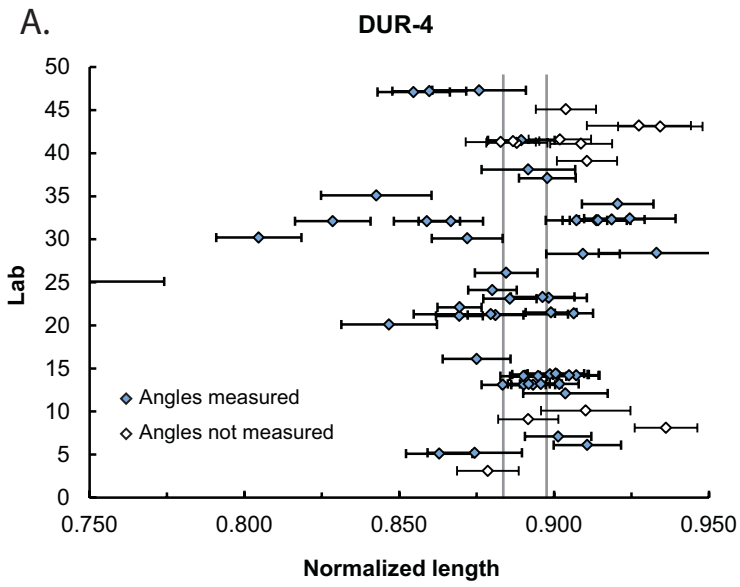


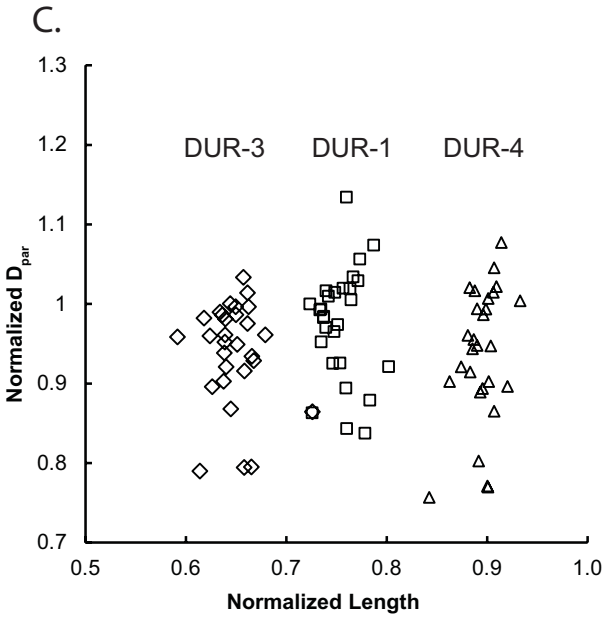
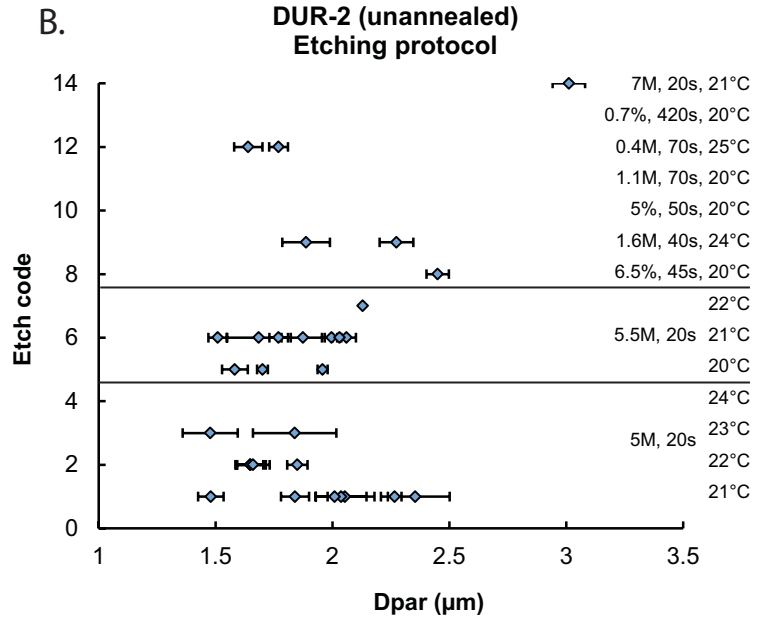
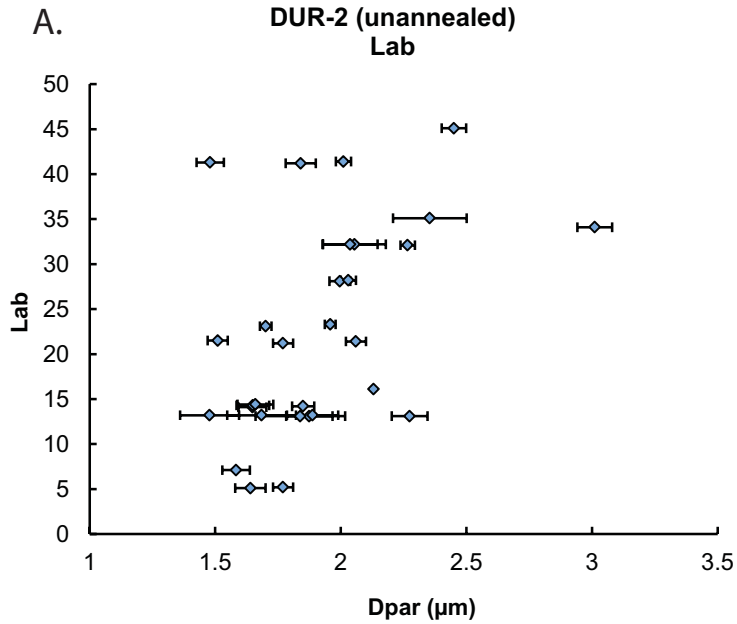












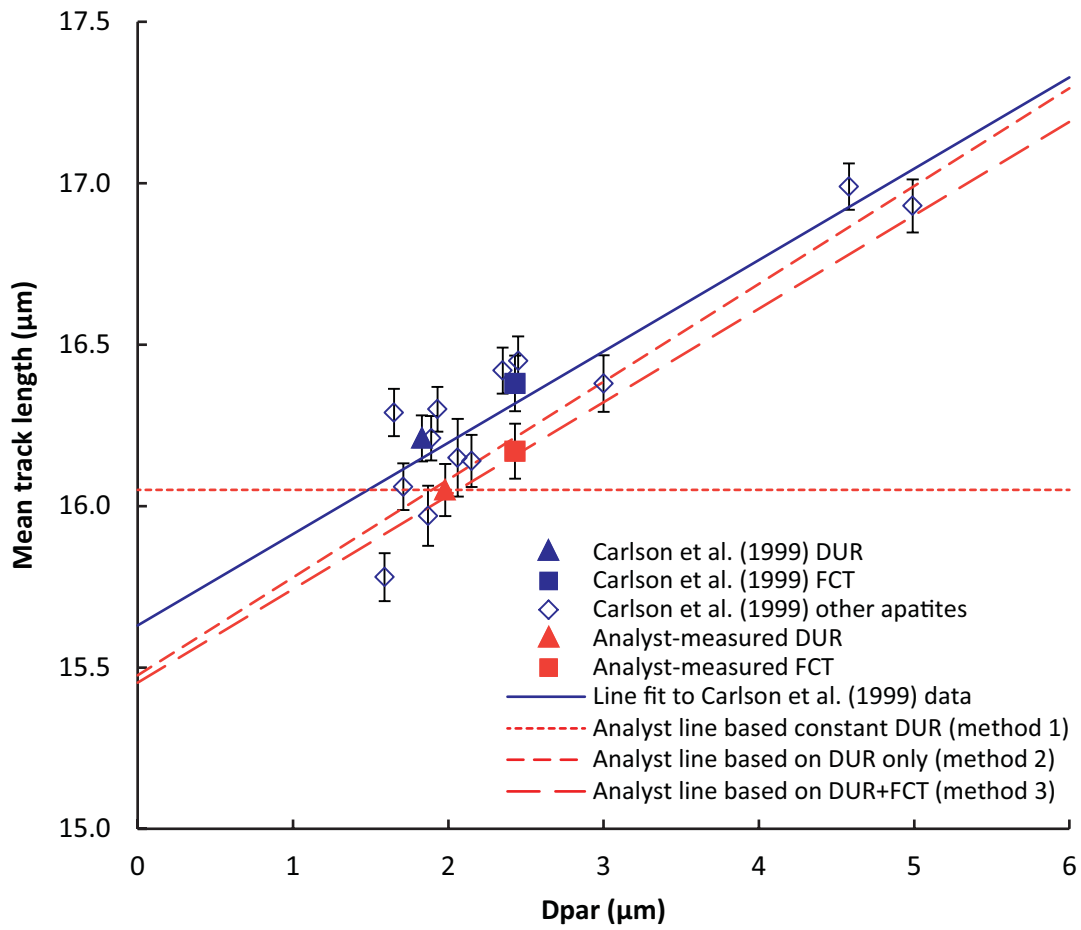


Table 1a: Survey responses for labs and analysts participating in experiment.

Lab ID	Analyst	Etch	Years	M/yr	M/yr (3 yr)	LED	Scope	Mag.	TINCLE used?	System	Standards measured
03	1	1	15.5	25	25	1	1	1600	N	2	N
05	1	12	2	20	20	1	1	1250	N	4	Internal i
	2	12	10	20	20	1	1	1250	N	4	Internal i
06	1	6	20	60	20	1	1	1250	Y	2	N
07	1	5	20	20	10	1	1	1250	?	2	N
08	1	6	3	80	80	?	2	?	N	1	N
09*	1	13	20	20	20	1	1	3840	N	3	DRi+FCi
10	1	4	14	55	35	1	1	1250	Y	2	N
12	1	?	?	?	?	?	?	?	?	?	?
13	1	6, 9, 3	24	300	300	1	1	1563	N	3	DR+FC
	2	6, 9, 3	19	300	300	1	1	1563	N	3	DR+FC
14	1	2	33	20	20	1	1	1250	N+Y	?	N
	2	2	26	2	2	1	1	1250	N+Y	?	N
	3	2	31	180	180	1	1	1250	N+Y	?	N
	4	2	15	180	180	1	1	1250	N	?	N
16	1	7	19	35	35	1	1	1250	N	2	FCs
21	A	6	0.5	2	0	1	1	1250	N	3	N
	B	6	4	15	13	1	1	1250	N	3	N
	C	6	0	0	0	1	1	1250	Y	3	N
	D	6	20	20	20	1	1	1250	N	3	N
	E	6	0	0	0	1	1	1250	Y	3	N
22	1	1	24	75	75	1	1	1600	N	3	Not recently
23	1	5	>1	>1	>1	1	1	100	N	1	DR s+i
	2	5	>1	>1	>1	1	1	100	N	1	DR s+i
	3	5	>1	>1	>1	1	1	100	N	1	DR s+i
24	1	1	>1	few	few	1	1	1000	N	3	Not suitable
25	1	1	6	37.5	37.5	1	1	1250	N	2	N
26	1	1	15	40	25	1	1	1000	N	2	N
28	1	6	17	30	30	1	1	1250	N	2	N
	2	6	5	19	9	1	1	1250	N	2	N
30	1	6	9	10	0	1	1	?	N	2	DRi Pisa
	2	6	0	0	0	2	1	?	N	2	N
32	1	1	38	100	17	1	1	1250	N	2	DR+FC

	2	1	?	?	?	?	1	1250	N	2	DR+FC
	3	1	?	?	?	?	1	1250	N	2	N
	4	1	0.01	0	0	?	1	1250	N	2	N
34	1	14	11	50	?	1	1	1250	N	2	N
35*	1	1	3	0	?	1	1	1250	N	2	N
37	1	6	0.1	0	0	1	1	1000	N	2	N
38	1	10	18	84	84	1	1	1250	N	2	DRi Pisa
39	1	6	10	20	20	1	1	1000	N	2	N
	2	6	0.1	0	0	1	1	1000	N	2	N
41	1	1	15	93	60	1	1	1250	N	2	N
	2	1	25	30	30	1	1	1250	N	2	N
	3	1	3	25	25	1	1	1250	N	2	FCs
	4	1	5	50	50	1	1	1250	N	2	DRs+FCs
	5	1	36	75	0	1	1	1600	N	2	N
	6	1	2	40	40	1	1	1600	N	2	Y
43	1	11	6	15	10	1	1	1500	N	3	DRs+DRi
	2	11	8	3	3	1	1	1500	N	3	N
45	1	8	11	40	50	3	1	1250	N	2	N
47	1	6	5	75	75	1	1	1000	N	1	DR+FC
	2	6	1	15	15	1	1	1000	N	1	DR+FC
	3	6	20	5	2	1	1	1600	N	1	DR

Question marks indicate no response provided.

Etch: Codes given in Table 1b;

Years: Number of years before experiment train in fission-track analysis;

M/yr: Estimated average number of track mounts measured per year over career;

M/yr (3 yrs): Estimated average over 3 years preceding experiment;

LED: 1=LED placed over track tips; 2=LED placed tangential to internal arc of track tips;

3=LED placed on opposite tangents of tip arcs on each end of track;

Scope: 1=air; 2=oil immersion;

Mag.: Scope magnification for measurements

System: 1=Autoscan; 2=FTStage; 3=other (custom system); 4=no computer (manual);

Standards measured: DR=Durango; FC=Fish Canyon; i=induced; s=spontaneous; Pisa=measured only during Ketcham et al. (2009) experiment; Y=yes (no details provided); N=none.

* Labs 9 and 35 experience predominantly or exclusively with zircon rather than apatite.

Table 1b: Etch codes and protocols, as specified by respondents

Etch Code	HNO ₃ (M)	HNO ₃ (%)	Time (s)	Temp (°C)	Notes
1	5		20	21	
2	5		20	22	
3	5		20	23	
4	5		20	24	
5	5.5		20	20	
6	5.5		20	21	
7	5.5		20	22	
8		6.5	45	20	
9	1.6		40	24	
10		5	50	20	
11	1.1		70	20	
12	0.4	2.5	70	25	
13		0.7	Up to 420	20	Variable etch time
14	7		20	21	

Table 2: Data for sample DUR-2.

Lab	Anal.	N_l	l_m (μm)	σ_l (μm)	ϕ_m ($^\circ$)	σ_ϕ ($^\circ$)	$l_{c,\text{fit}}$ (μm)	$l_{a,\text{fit}}$ (μm)	σ_e (μm)	$l_{c,\text{mod(B03)}}$ (μm)	$l_{c,\text{mod(C99)}}$ (μm)	D_{par} (μm)	Notes
03	1	100	16.07(09)	0.87	--	--	--	--	--	--	--	--	
05	1	100	16.38(08)	0.82	54	20	16.78(18)	16.16(12)	0.80	16.55(06)	16.63(06)	1.64(03)	
05	2	100	16.23(09)	0.87	45	23	16.24(14)	16.21(14)	0.87	16.39(07)	16.46(07)	1.77(02)	
06	1	100	15.25(09)	0.90	56	18	15.55(21)	15.09(12)	0.89	15.68(07)	15.82(06)	--	
07	1	101	15.95(07)	0.70	54	14	16.28(24)	15.78(14)	0.69	16.22(05)	16.32(05)	1.58(03)	
08	1	211	15.34(09)	1.33	--	--	--	--	--	--	--	--	
09	1	50	16.43(11)	0.75	--	--	--	--	--	--	--	--	
10	1	100	15.89(09)	0.92	--	--	--	--	--	--	--	--	
10	2	100	15.87(08)	0.84	59	16	16.04(26)	15.80(12)	0.84	16.17(06)	16.28(06)	--	Repeat
12	1	100	15.29(12)	1.18	51	23	15.62(16)	15.06(12)	1.17	15.68(09)	15.81(09)	--	
13	1	200	16.57(06)	0.84	59	16	17.30(18)	16.30(08)	0.81	16.72(05)	16.79(04)	1.87(05)	Etch 6
13	1	205	16.84(05)	0.78	55	17	17.48(15)	16.51(09)	0.74	16.92(04)	16.97(04)	2.27(04)	Etch 9
13	1	203	16.49(07)	0.94	58	15	17.12(19)	16.24(09)	0.92	16.65(05)	16.73(05)	1.84(09)	Etch 3
13	2	200	16.59(06)	0.80	57	16	17.25(18)	16.28(09)	0.76	16.72(04)	16.79(04)	1.68(07)	Etch 6
13	2	200	16.80(07)	0.94	56	17	17.20(16)	16.60(09)	0.93	16.87(05)	16.93(05)	1.89(05)	Etch 9
13	2	200	16.77(06)	0.91	57	17	17.35(17)	16.51(09)	0.89	16.86(05)	16.92(05)	1.48(06)	Etch 3
14	1	74	15.95(10)	0.83	59	15	16.35(32)	15.79(14)	0.83	16.24(07)	16.35(07)	--	TINT
14	1	27	16.22(18)	0.89	53	17	17.13(41)	15.71(24)	0.83	16.44(14)	16.52(13)	--	TINCLE
14	1	100	16.02(09)	0.87	58	16	16.68(25)	15.74(12)	0.83	16.29(06)	16.39(06)	1.65(03)	Combined
14	2	88	15.94(08)	0.73	59	14	16.18(30)	15.84(14)	0.72	16.23(06)	16.34(05)	--	TINT
14	2	32	16.38(13)	0.74	61	17	16.46(43)	16.35(20)	0.74	16.56(10)	16.64(09)	--	TINCLE
14	2	120	16.06(07)	0.76	59	14	16.21(25)	16.00(12)	0.75	16.32(05)	16.42(05)	1.85(02)	Combined
14	3	129	15.45(11)	1.28	59	17	15.95(22)	15.25(10)	1.27	15.87(08)	16.01(07)	--	TINT
14	3	41	15.86(16)	1.00	57	18	16.75(38)	15.45(19)	0.95	16.17(12)	16.28(11)	--	TINCLE
14	3	170	15.55(09)	1.23	59	17	16.18(19)	15.29(09)	1.21	15.94(07)	16.07(06)	1.65(03)	Combined
14	4	150	15.39(08)	0.93	57	15	15.51(21)	15.33(11)	0.93	15.80(06)	15.94(05)	1.66(04)	

16	1	100	16.48(07)	0.72	60	17	16.78(24)	16.37(12)	0.71	16.64(05)	16.71(05)	2.13(00)	
20	1	94	15.53(10)	0.92	62	12	15.66(35)	15.49(13)	0.92	15.94(07)	16.08(07)	--	
21	1	232	15.93(06)	0.88	49	21	16.09(11)	15.81(09)	0.88	16.17(05)	16.26(04)	--	
21	2	256	15.56(05)	0.87	51	18	15.94(12)	15.31(08)	0.86	15.90(04)	16.02(04)	1.77(02)	
21	3	125	14.45(15)	1.63	51	20	14.32(15)	14.54(12)	1.63	15.01(12)	15.19(11)	--	
21	4	253	16.24(06)	0.88	58	20	16.42(12)	16.16(07)	0.88	16.45(04)	16.53(04)	2.06(02)	
21	5	308	14.66(05)	0.92	54	19	14.90(11)	14.52(07)	0.91	15.22(04)	15.39(04)	1.51(02)	
22	1	99	15.46(07)	0.69	60	14	15.55(29)	15.43(13)	0.69	15.87(05)	16.01(05)	--	
23	1	100	15.83(06)	0.58	63	13	15.97(34)	15.78(12)	0.58	16.16(04)	16.28(04)	1.70(01)	
23	2	99	15.82(07)	0.74	60	19	15.85(22)	15.81(11)	0.75	16.13(06)	16.24(05)	--	
23	3	100	15.78(07)	0.70	57	18	16.12(21)	15.62(12)	0.68	16.10(05)	16.21(05)	1.96(01)	
24	1	102	16.11(08)	0.79	61	14	16.35(30)	16.03(12)	0.79	16.36(06)	16.46(05)	--	
25	1	100	13.59(19)	1.85	57	16	14.76(27)	13.11(12)	1.81	14.47(13)	14.73(12)	--	
26	1	100	15.74(08)	0.76	57	17	16.18(24)	15.53(12)	0.75	16.07(06)	16.19(05)	--	
28	1	100	15.33(11)	1.13	52	19	15.42(18)	15.27(13)	1.13	15.71(09)	15.84(09)	2.00(02)	
28	2	100	14.67(16)	1.64	54	24	14.74(16)	14.62(11)	1.63	15.20(13)	15.37(12)	2.03(01)	
30	1	101	15.97(07)	0.72	62	14	16.39(30)	15.84(11)	0.71	16.27(05)	16.38(05)	--	
30	2	104	15.98(11)	1.09	64	12	15.48(33)	16.12(12)	1.09	16.28(08)	16.39(07)	--	
32	1	101	16.01(07)	0.70	61	14	15.92(29)	16.04(13)	0.69	16.28(05)	16.39(05)	--	Aliquot a
32	1	103	16.13(08)	0.81	57	18	16.51(21)	15.96(11)	0.79	16.37(06)	16.46(06)	2.27(01)	Aliquot b
32	1	104	16.52(10)	0.99	57	18	16.82(21)	16.38(12)	0.98	16.66(07)	16.73(07)	--	Aliquot c
32	2	102	15.72(09)	0.87	53	19	16.35(19)	15.33(12)	0.82	16.04(06)	16.15(06)	2.05(06)	Aliquot a
32	2	103	15.88(07)	0.75	56	19	16.01(20)	15.81(12)	0.74	16.16(06)	16.27(05)	--	Aliquot b
32	2	102	15.68(08)	0.83	55	19	16.30(20)	15.37(12)	0.79	16.02(06)	16.14(06)	2.04(05)	Aliquot c
32	3	100	15.98(09)	0.86	62	16	16.24(26)	15.89(11)	0.86	16.27(07)	16.37(06)	--	
32	4	100	15.39(11)	1.12	55	17	15.13(21)	15.54(14)	1.12	15.77(09)	15.90(09)	--	
34	1	100	15.61(10)	0.96	59	16	15.84(25)	15.53(12)	0.96	15.99(07)	16.11(07)	3.01(03)	
35	1	56	15.82(15)	1.11	53	19	16.63(27)	15.35(17)	1.05	16.13(11)	16.24(10)	2.35(07)	
37	1	50	15.88(08)	0.57	55	23	16.09(24)	15.77(16)	0.56	16.16(06)	16.26(06)	--	

38	1	100	15.88(10)	0.97	56	21	16.14(19)	15.73(12)	0.97	16.16(08)	16.26(07)	--	
39	1	80	16.45(09)	0.80	--	--	--	--	--	--	--	--	
39	2	47	15.54(16)	1.42	--	--	--	--	--	--	--	--	
41	1	100	16.00(09)	0.88	--	--	--	--	--	--	--	--	
41	2	100	16.25(07)	0.70	--	--	--	--	--	--	--	1.84(03)	
41	3	100	15.87(10)	1.01	57	15	15.99(25)	15.82(13)	1.01	16.17(08)	16.28(07)	1.48(03)	
41	4	100	16.61(07)	0.75	61	12	16.82(35)	16.54(13)	0.74	16.73(06)	16.81(05)	2.01(02)	
41	5	100	16.08(08)	0.84	59	13	16.44(30)	15.95(13)	0.83	16.34(06)	16.44(06)	--	Cf
41	6	100	15.90(10)	1.00	61	10	16.43(41)	15.73(15)	0.99	16.21(07)	16.33(07)	--	
43	1	100	15.29(14)	1.37	--	--	--	--	--	--	--	--	
43	2	99	15.27(13)	1.26	--	--	--	--	--	--	--	--	
45	1	100	16.43(09)	0.93	--	--	--	--	--	--	--	2.45(02)	
47	1	100	16.05(08)	0.81	53	22	16.70(18)	15.66(12)	0.75	16.30(06)	16.40(06)	--	
47	2	100	15.87(08)	0.84	53	22	16.53(18)	15.47(12)	0.78	16.16(07)	16.26(06)	--	
47	3	104	15.67(07)	0.75	56	18	16.05(21)	15.49(12)	0.74	16.02(05)	16.14(05)	--	

Table 3: Data for sample DUR-4.

Lab	Anal.	N_1	l_m μm	σ_l μm	ϕ_m $^\circ$	σ_ϕ $^\circ$	$l_{c,fit}$ μm	$l_{a,fit}$ μm	σ_e μm	$l_{c,mod(B03)}$ μm	$l_{c,mod(C99)}$ μm	D_{par} μm	Notes
03	1	100	14.12(08)	0.80	--	--	--	--	--	--	--	--	
05	1	100	14.13(09)	0.88	53	17	14.88(21)	13.74(12)	0.82	14.83(06)	15.03(06)	1.48(02)	
05	2	100	14.19(12)	1.24	53	17	14.42(20)	14.06(13)	1.23	14.85(10)	15.05(09)	1.63(02)	
06	1	100	13.89(08)	0.83	60	19	14.87(25)	13.52(11)	0.76	14.71(06)	14.94(05)	--	
07	1	105	14.38(09)	0.88	56	14	15.60(30)	13.85(13)	0.81	15.05(06)	15.25(05)	1.59(02)	
08	1	175	14.36(08)	1.03	--	--	--	--	--	--	--	--	
09	1	50	14.65(08)	0.60	--	--	--	--	--	--	--	--	
10	1	100	14.46(11)	1.15	--	--	--	--	--	--	--	--	
12	1	100	13.82(10)	1.04	60	18	15.22(25)	13.32(11)	0.92	14.67(07)	14.90(06)	--	
13	1	202	14.80(06)	0.83	59	17	15.94(18)	14.37(08)	0.74	15.39(04)	15.57(04)	1.67(03)	Etch 6
13	1	203	14.88(06)	0.82	56	19	15.70(15)	14.50(08)	0.75	15.42(04)	15.59(04)	2.08(05)	Etch 9
13	1	202	14.68(06)	0.83	61	15	15.78(22)	14.34(08)	0.78	15.32(04)	15.51(04)	1.83(11)	Etch 3
13	2	200	14.86(06)	0.79	58	16	15.53(18)	14.57(08)	0.76	15.41(04)	15.58(04)	1.50(06)	Etch 6
13	2	200	15.15(05)	0.73	56	17	15.65(16)	14.90(09)	0.71	15.61(04)	15.76(04)	1.70(04)	Etch 9
13	2	200	14.96(06)	0.80	33	141	15.60(22)	14.73(09)	0.78	15.51(04)	15.68(04)	1.19(07)	Etch 3
14	1	109	14.27(07)	0.75	60	16	14.87(26)	14.04(11)	0.73	14.99(05)	15.20(05)	--	TINT
14	1	41	14.22(14)	0.88	56	14	14.45(40)	14.12(19)	0.88	14.93(11)	15.15(10)	--	TINCLE
14	1	150	14.26(06)	0.79	59	15	14.75(22)	14.07(10)	0.78	14.97(05)	15.18(04)	1.45(03)	Combined
14	2	63	14.43(08)	0.60	58	13	15.01(39)	14.19(17)	0.58	15.10(06)	15.30(05)	--	TINT
14	2	38	14.81(10)	0.63	59	15	15.28(43)	14.62(20)	0.62	15.38(07)	15.56(07)	--	TINCLE
14	2	101	14.57(06)	0.64	58	14	15.10(29)	14.36(13)	0.62	15.20(05)	15.40(04)	1.60(03)	Combined
14	3	90	13.89(09)	0.89	57	16	14.71(27)	13.53(13)	0.85	14.68(07)	14.91(06)	--	TINT
14	3	70	14.18(14)	1.13	58	19	15.74(29)	13.56(13)	0.98	14.92(09)	15.13(08)	--	TINCLE
14	3	160	14.01(08)	1.01	57	17	15.20(20)	13.52(09)	0.92	14.78(05)	15.01(05)	1.27(04)	Combined
14	4	150	13.86(07)	0.84	60	16	14.60(23)	13.61(09)	0.82	14.70(05)	14.93(04)	1.28(04)	
16	1	100	14.42(09)	0.88	57	18	15.56(25)	13.92(12)	0.79	15.08(06)	15.28(06)	--	

20	1	109	13.15(12)	1.30	61	11	13.26(36)	13.11(14)	1.30	14.20(09)	14.50(08)	--	
21	A	255	13.85(06)	1.03	56	18	14.13(13)	13.71(08)	1.02	14.62(05)	14.84(05)	--	
21	B	212	13.71(07)	0.95	52	20	14.49(13)	13.23(08)	0.88	14.47(05)	14.69(04)	--	
21	C	125	12.71(18)	1.97	48	24	11.98(12)	13.37(12)	1.92	13.60(15)	13.85(14)	--	
21	D	273	14.72(05)	0.86	54	21	15.39(11)	14.35(07)	0.81	15.28(04)	15.45(04)	--	
21	E	268	13.18(06)	0.91	58	16	13.68(16)	12.98(07)	0.90	14.16(04)	14.44(04)	--	
22	1	120	13.45(06)	0.60	58	15	13.65(24)	13.36(12)	0.60	14.35(04)	14.61(04)	--	
23	1	100	14.02(07)	0.68	60	13	15.48(39)	13.54(13)	0.59	14.82(04)	15.05(04)	1.61(01)	
23	2	99	14.21(10)	0.97	60	18	14.58(24)	14.07(11)	0.96	14.94(08)	15.16(07)	--	
23	3	100	14.14(08)	0.81	57	18	14.56(22)	13.95(11)	0.79	14.86(06)	15.07(06)	1.93(01)	
24	1	104	14.18(06)	0.64	75	30	14.75(25)	13.99(10)	0.62	14.94(04)	15.16(04)	--	
25	1	100	10.08(22)	2.19	55	18	9.72(19)	10.30(13)	2.19	12.06(14)	12.53(14)	--	
26	1	100	13.92(08)	0.79	53	18	14.63(20)	13.51(12)	0.74	14.65(06)	14.87(05)	--	
28	1	100	13.94(09)	0.91	56	19	14.57(21)	13.63(12)	0.88	14.70(07)	14.92(06)	2.04(02)	
28	2	100	13.68(14)	1.37	55	21	14.78(20)	13.14(11)	1.29	14.51(09)	14.75(08)	2.04(02)	
30	1	105	13.93(09)	0.93	66	15	14.40(33)	13.81(10)	0.93	14.79(06)	15.04(06)	--	
30	2	100	12.86(11)	1.11	61	16	13.30(27)	12.71(12)	1.10	13.96(08)	14.26(08)	--	
32	1	100	13.87(08)	0.83	59	17	14.75(25)	13.55(11)	0.77	14.69(06)	14.93(05)	2.26(03)	aliquot a
32	1	101	13.86(09)	0.86	59	15	14.59(27)	13.58(12)	0.83	14.68(06)	14.91(06)	--	aliquot b
32	1	101	13.69(10)	1.01	58	17	14.23(24)	13.46(12)	0.99	14.53(08)	14.78(07)	--	aliquot c
32	2	101	14.26(08)	0.78	54	19	15.07(20)	13.82(12)	0.71	14.92(05)	15.12(05)	2.15(05)	aliquot a
32	2	101	14.51(09)	0.88	53	19	14.87(19)	14.30(12)	0.86	15.10(07)	15.28(06)	2.24(04)	aliquot b
32	2	101	14.33(07)	0.72	55	19	15.29(21)	13.87(11)	0.61	15.00(05)	15.20(04)	2.19(05)	aliquot c
32	3	110	14.68(08)	0.88	56	18	15.47(21)	14.31(11)	0.83	15.27(06)	15.45(06)	--	
32	4	100	14.23(11)	1.13	63	20	14.15(22)	14.26(11)	1.13	14.95(09)	15.16(08)	--	
34	1	100	14.37(09)	0.92	59	18	15.32(24)	14.01(11)	0.86	15.06(07)	15.26(06)	2.70(03)	
35	1	111	13.33(14)	1.49	60	15	14.30(30)	13.00(11)	1.46	14.34(09)	14.61(08)	1.78(04)	
37	1	50	14.26(07)	0.51	52	24	14.08(22)	14.37(17)	0.50	14.85(08)	15.03(08)	--	
38	1	100	14.16(12)	1.21	50	20	14.59(17)	13.87(13)	1.19	14.80(09)	14.99(09)	--	

39	1	80	14.98(08)	0.71	--	--	--	--	--	--	--	--	
41	1	100	14.54(08)	0.76	--	--	--	--	--	--	--	--	
41	2	100	14.43(08)	0.82	--	--	--	--	--	--	--	1.87(02)	
41	2	100	14.42(08)	0.80	--	--	--	--	--	--	--	--	Cf
41	3	100	14.01(09)	0.87	63	15	15.42(35)	13.63(11)	0.80	14.84(06)	15.07(05)	1.51(02)	
41	4	100	14.73(07)	0.69	62	12	15.67(41)	14.47(13)	0.67	15.36(05)	15.55(04)	1.92(02)	
41	5	100	14.31(09)	0.86	60	15	15.26(30)	13.99(11)	0.82	15.03(06)	15.24(06)	--	Cf
41	6	101	14.34(08)	0.77	63	11	15.25(44)	14.10(13)	0.76	15.08(05)	15.30(05)	--	
43	1	100	14.28(10)	1.04	--	--	--	--	--	--	--	--	
43	2	100	14.16(13)	1.27	--	--	--	--	--	--	--	--	
45	1	100	14.85(08)	0.79	--	--	--	--	--	--	--	2.32(02)	
47	1	100	13.72(09)	0.94	59	20	14.34(21)	13.45(11)	0.90	14.55(07)	14.79(07)	--	
47	2	100	13.64(09)	0.95	59	20	14.23(21)	13.39(11)	0.92	14.49(07)	14.73(07)	--	
47	3	106	13.73(12)	1.03	61	17	14.37(25)	13.51(11)	1.01	14.60(07)	14.85(07)	--	

Table 4: Data for sample DUR-1.

Lab	Anal.	N _l	I _m (μm)	σ _l (μm)	φ _m (°)	σ _φ (°)	I _{c,fit} (μm)	I _{a,fit} (μm)	σ _e (μm)	I _{c,mod(B03)} (μm)	I _{c,mod(C99)} (μm)	D _{par} (μm)	Notes
03	1	100	12.32(10)	0.95	--	--	--	--	--	--	--	--	
05	1	100	12.45(10)	0.96	50	19	13.59(19)	11.75(12)	0.81	13.50(06)	13.79(06)	1.86(02)	
05	2	100	12.55(16)	1.56	44	23	12.76(14)	12.34(14)	1.56	13.40(14)	13.66(13)	1.87(02)	
06	1	100	11.85(09)	0.91	54	22	12.94(20)	11.28(11)	0.77	13.09(06)	13.43(06)	--	
07	1	100	11.70(09)	0.88	59	16	13.22(29)	11.21(11)	0.76	13.11(06)	13.49(05)	1.57(04)	
08	1	221	12.19(08)	1.16	--	--	--	--	--	--	--	--	
09	1	50	12.35(14)	0.98	--	--	--	--	--	--	--	--	
10	1	100	11.94(09)	0.90	--	--	--	--	--	--	--	--	
12	1	93	12.10(10)	0.98	52	22	12.98(19)	11.55(12)	0.88	13.22(07)	13.54(07)	--	
13	1	210	12.18(06)	0.91	59	17	13.81(19)	11.60(07)	0.74	13.44(04)	13.78(03)	1.79(03)	Etch 6
13	1	201	12.45(07)	0.97	55	19	13.95(15)	11.77(08)	0.77	13.59(04)	13.90(04)	2.21(06)	Etch 9
13	1	204	12.16(07)	0.97	60	15	14.15(23)	11.54(08)	0.81	13.45(04)	13.80(04)	1.81(10)	Etch 3
13	2	200	12.60(06)	0.80	55	16	13.55(18)	12.13(09)	0.73	13.67(04)	13.98(04)	1.51(04)	Etch 6
13	2	200	12.38(07)	0.97	57	16	14.00(19)	11.76(08)	0.82	13.57(04)	13.90(04)	1.86(06)	Etch 9
13	2	200	12.18(06)	0.85	58	15	13.19(20)	11.79(08)	0.80	13.43(04)	13.77(04)	1.27(06)	Etch 3
14	1	74	12.21(12)	1.01	57	19	13.91(29)	11.51(13)	0.83	13.43(08)	13.76(07)	--	TINT
14	1	31	11.93(14)	0.75	62	13	13.43(67)	11.50(20)	0.66	13.31(09)	13.68(08)	--	TINCLE
14	1	105	12.12(09)	0.95	58	17	13.84(27)	11.49(11)	0.78	13.39(06)	13.74(05)	1.56(03)	Combined
14	2	105	12.16(07)	0.71	61	21	12.78(22)	11.92(10)	0.67	13.41(05)	13.75(05)	--	TINT
14	2	13	12.67(26)	0.90	54	22	13.23(53)	12.36(33)	0.86	13.70(18)	13.98(17)	--	TINCLE
14	2	118	12.21(07)	0.75	60	21	12.86(20)	11.96(10)	0.71	13.44(05)	13.78(05)	1.56(03)	Combined
14	3	106	12.15(09)	0.92	59	17	12.79(24)	11.90(11)	0.90	13.40(06)	13.75(06)	--	TINT
14	3	46	12.26(12)	0.80	59	19	13.07(35)	11.92(17)	0.74	13.47(08)	13.80(08)	--	TINCLE
14	3	152	12.18(07)	0.88	59	18	12.88(20)	11.90(09)	0.85	13.42(05)	13.76(05)	1.45(05)	Combined
14	4	150	11.98(06)	0.77	61	17	13.06(23)	11.62(09)	0.70	13.32(04)	13.68(04)	1.39(04)	
16	1	100	12.36(09)	0.90	56	19	13.50(22)	11.81(11)	0.78	13.50(06)	13.82(05)	2.12(00)	

20	1	98	11.62(10)	0.97	62	14	13.61(41)	11.11(11)	0.87	13.10(06)	13.50(06)	--	
21	A	252	12.19(06)	0.88	53	18	12.84(13)	11.82(08)	0.84	13.33(04)	13.65(04)	--	
21	B	208	11.93(06)	0.91	48	20	12.86(12)	11.23(09)	0.77	13.03(04)	13.35(04)	1.83(02)	
21	C	125	11.59(13)	1.49	46	23	12.42(14)	10.89(11)	1.41	12.73(10)	13.06(10)	--	
21	D	268	12.53(06)	1.01	54	21	14.08(13)	11.77(07)	0.76	13.63(04)	13.93(03)	2.12(04)	
21	E	259	10.77(07)	1.06	57	17	11.48(15)	10.44(07)	1.03	12.37(05)	12.81(04)	1.50(02)	
22	1	100	11.51(10)	0.95	64	17	12.83(33)	11.15(11)	0.89	13.03(06)	13.43(06)	--	
23	1	100	11.83(09)	0.85	55	18	12.25(22)	11.62(12)	0.84	13.09(07)	13.44(07)	1.64(01)	
23	2	100	11.96(11)	1.06	54	20	13.51(22)	11.21(11)	0.84	13.20(07)	13.53(06)	--	
23	3	100	11.85(07)	0.72	55	19	12.57(21)	11.49(12)	0.66	13.10(05)	13.45(05)	1.91(01)	
24	1	112	12.14(06)	0.64	59	16	13.04(26)	11.81(11)	0.58	13.41(04)	13.75(04)	--	
25	1	100	11.09(14)	1.36	59	19	12.23(26)	10.67(11)	1.31	12.69(08)	13.12(07)	--	
26	1	100	11.76(09)	0.89	55	17	13.32(26)	11.05(12)	0.71	13.06(05)	13.42(05)	--	
28	3	100	11.72(12)	1.08	57	18	13.28(26)	11.09(11)	0.94	13.07(07)	13.44(06)	2.01(02)	
28	4	100	11.54(11)	1.06	52	23	12.42(17)	11.02(11)	0.96	12.81(07)	13.16(07)	2.18(02)	
30	1	108	11.13(09)	0.96	63	14	13.15(40)	10.65(10)	0.84	12.77(06)	13.21(05)	--	
30	2	100	9.97(12)	1.21	63	11	9.00(30)	10.31(15)	1.19	12.06(08)	12.59(07)	--	
0	2	30	10.60(17)	0.91	64	13	12.76(95)	10.15(20)	0.81	12.41(10)	12.90(09)	--	
	(repeat)												
32	1	103	11.77(07)	0.70	56	20	12.30(21)	11.50(12)	0.67	13.04(05)	13.40(06)	--	aliquot a
32	1	102	11.97(08)	0.83	57	20	12.92(22)	11.56(11)	0.75	13.23(05)	13.58(05)	2.29(03)	aliquot b
32	1	104	11.84(08)	0.82	58	18	12.73(24)	11.49(11)	0.76	13.17(06)	13.53(06)	2.18(03)	aliquot c
32	2	102	12.00(10)	0.97	35	24	13.34(26)	11.42(12)	0.86	13.26(06)	13.61(06)	2.09(05)	aliquot a
32	2	102	12.13(08)	0.82	55	20	13.37(21)	11.55(11)	0.64	13.33(05)	13.66(04)	2.07(05)	aliquot b
32	2	102	11.93(09)	0.94	54	20	13.43(22)	11.21(11)	0.72	13.17(06)	13.51(05)	--	aliquot c
32	3	0	.00(00)	0.00	--	--	--	--	--	--	--	--	
32	4	100	10.79(13)	1.31	56	14	10.61(24)	10.89(15)	1.31	12.40(10)	12.84(09)	--	
34	1	100	12.52(11)	1.06	58	16	14.65(32)	11.76(11)	0.88	13.68(07)	14.01(06)	2.77(03)	
35	1	57	11.84(12)	0.90	60	18	12.88(32)	11.40(15)	0.71	13.14(07)	13.50(07)	2.39(07)	
37	1	50	12.22(11)	0.74	51	30	12.32(19)	12.15(16)	0.74	13.22(11)	13.50(12)	--	
38	1	100	11.29(15)	1.55	51	22	12.31(19)	10.65(12)	1.47	12.68(09)	13.04(09)	--	
39	1	80	12.12(09)	0.90	--	--	--	--	--	--	--	--	
39	0	0	.00(00)	0.00	--	--	--	--	--	--	--	--	
41	1	101	12.05(09)	0.91	--	--	--	--	--	--	--	--	
41	2	125	12.02(09)	1.03	--	--	--	--	--	--	--	1.87(03)	
41	2	125	12.18(08)	0.87	--	--	--	--	--	--	--	--	Cf

41	3	100	11.96(10)	1.01	62	16	14.06(34)	11.39(10)	0.84	13.34(06)	13.71(05)	1.37(02)	
41	4	100	12.40(08)	0.82	63	11	15.07(58)	11.83(12)	0.69	13.69(05)	14.03(05)	1.86(02)	
41	5	100	11.43(10)	1.00	61	16	12.43(30)	11.12(11)	0.96	12.95(07)	13.35(06)	--	Cf
41	6	100	12.08(07)	0.72	64	11	13.26(47)	11.81(12)	0.68	13.47(05)	13.84(05)	--	
43	1	100	12.26(10)	0.98	--	--	--	--	--	--	--	--	
43	2	99	12.23(14)	1.38	--	--	--	--	--	--	--	--	
45	1	100	11.89(10)	1.00	--	--	--	--	--	--	--	2.45(02)	

Table 5: Data for sample DUR-3.

Lab	Anal.	N_l	I_m (μm)	σ_l (μm)	ϕ_m ($^\circ$)	σ_ϕ ($^\circ$)	N_{cell}	$I_{c,\text{fit}}$ (μm)	$I_{a,\text{fit}}$ (μm)	σ_e (μm)	$I_{c,\text{mod(B03)}}$ (μm)	$I_{c,\text{mod(C99)}}$ (μm)	D_{par} (μm)	Notes
03	1	100	10.50(10)	0.97	--	--	--	--	--	--	--	--	--	
05	1	100	10.45(13)	1.27	48	18	99	12.38(21)	9.35(12)	0.91	12.02(07)	12.46(06)	1.48(02)	
05	2	100	10.69(15)	1.50	47	21	99	12.19(18)	9.68(12)	1.21	12.16(09)	12.56(08)	1.62(02)	
06	1	100	10.43(10)	0.99	50	16	100	11.87(21)	9.57(12)	0.78	11.98(05)	12.43(05)	--	
07	1	102	9.44(18)	1.82	56	18	90	11.57(27)	9.23(12)	0.97	11.81(06)	12.30(06)	1.52(02)	
08	1	234	10.22(09)	1.35	--	--	--	--	--	--	--	--	--	
09	1	50	11.23(16)	1.13	--	--	--	--	--	--	--	--	--	
10	1	100	10.50(12)	1.18	--	--	--	--	--	--	--	--	--	
12	1	99	9.76(14)	1.42	57	19	93	11.30(26)	9.46(12)	0.91	11.86(06)	12.37(06)	--	
13	1	204	10.60(09)	1.27	55	18	199	12.65(18)	9.87(08)	0.83	12.30(04)	12.75(04)	1.84(03)	Etch 6
13	1	204	11.14(08)	1.17	49	19	203	12.74(14)	10.21(08)	0.86	12.51(05)	12.89(04)	2.22(02)	Etch 9
13	1	200	10.56(09)	1.29	54	17	199	12.80(20)	9.65(08)	1.04	12.24(05)	12.69(05)	1.69(13)	Etch 3
13	2	200	10.78(12)	1.63	51	18	194	13.11(18)	9.82(08)	0.98	12.40(05)	12.82(05)	1.66(04)	Etch 6
13	2	200	10.94(10)	1.36	51	18	196	12.95(17)	10.01(08)	0.93	12.46(05)	12.87(04)	1.79(06)	Etch 9
13	2	175	10.68(09)	1.17	53	15	173	12.55(22)	9.91(09)	0.89	12.29(05)	12.73(04)	1.46(07)	Etch 3
14	1	118	10.65(10)	1.07	54	17	117	12.43(23)	9.89(11)	0.78	12.26(05)	12.70(05)	--	TINT
14	1	34	10.89(21)	1.19	56	19	34	12.25(38)	10.23(20)	1.05	12.40(13)	12.83(12)	--	TINCLE
14	1	152	10.70(09)	1.10	54	18	151	12.38(20)	9.97(09)	0.85	12.29(05)	12.73(05)	1.42(03)	Combined
14	2	85	10.60(13)	1.18	52	17	84	12.65(29)	9.73(13)	0.67	12.22(05)	12.66(05)	--	TINT
14	2	17	11.12(22)	0.89	50	22	17	12.26(41)	10.36(28)	0.64	12.44(11)	12.81(11)	--	TINCLE
14	2	102	10.69(11)	1.15	52	18	101	12.53(23)	9.84(12)	0.68	12.26(05)	12.69(04)	1.47(03)	Combined
14	3	119	10.14(16)	1.70	55	20	115	12.72(23)	9.29(10)	1.03	12.07(07)	12.54(06)	--	TINT
14	3	34	10.57(19)	1.09	55	20	34	12.14(41)	9.85(19)	0.94	12.19(11)	12.64(10)	--	TINCLE
14	3	153	10.24(13)	1.59	55	20	149	12.62(20)	9.41(09)	1.02	12.10(06)	12.56(05)	1.31(04)	Combined
14	4	150	9.93(11)	1.30	56	16	147	11.95(26)	9.27(09)	0.96	11.90(05)	12.41(04)	1.44(04)	
16	1	100	10.84(11)	1.14	53	20	100	13.06(24)	9.82(11)	0.74	12.38(06)	12.80(05)	--	

20	1	84	10.09(09)	0.86	56	13	84	11.40(38)	9.57(14)	0.79	11.92(06)	12.43(05)	--	
21	A	277	10.46(06)	0.96	55	15	277	12.65(20)	9.62(07)	0.73	12.15(03)	12.62(03)	--	
21	B	232	9.94(08)	1.25	49	19	231	11.96(14)	8.82(07)	0.84	11.70(04)	12.18(03)	--	
21	C	125	10.02(13)	1.46	51	23	123	11.25(16)	9.40(10)	1.25	11.82(08)	12.28(08)	--	
21	D	278	10.38(10)	1.69	53	21	262	12.52(13)	9.69(07)	0.86	12.22(04)	12.65(03)	--	
21	E	276	9.45(06)	1.01	54	19	276	10.71(13)	8.83(07)	0.87	11.48(04)	12.01(04)	--	
22	1	101	9.74(11)	1.07	54	16	101	12.23(33)	8.76(11)	0.78	11.71(04)	12.23(04)	--	
23	1	100	9.79(10)	0.96	60	14	100	11.79(41)	9.21(11)	0.84	11.85(05)	12.39(04)	1.67(01)	
23	2	100	9.90(11)	1.09	50	21	100	10.88(18)	9.26(12)	0.98	11.61(07)	12.08(08)	--	
23	3	100	10.09(11)	1.13	55	18	100	11.39(24)	9.52(11)	1.02	11.92(07)	12.41(06)	1.88(01)	
24	1	104	10.18(14)	1.46	63	26	97	12.74(31)	9.58(11)	0.71	12.15(05)	12.62(05)	--	
25	1	50	6.78(23)	1.64	53	16	50	7.69(40)	6.35(18)	1.61	10.74(08)	11.31(08)	--	
26	1	100	10.35(11)	1.07	54	20	100	12.25(23)	9.46(11)	0.77	12.02(05)	12.49(05)	--	
28	1	100	10.14(12)	1.22	54	21	98	11.81(21)	9.44(11)	0.86	11.93(06)	12.40(06)	2.02(02)	
28	2	100	9.53(18)	1.80	54	21	90	11.77(23)	9.07(12)	0.98	11.80(07)	12.29(06)	2.02(02)	
30	1	107	10.40(08)	0.86	60	14	107	12.30(41)	9.86(11)	0.75	12.22(05)	12.71(04)	--	
30	2	100	9.95(08)	0.85	61	13	100	10.43(38)	9.79(13)	0.84	11.95(06)	12.48(05)	--	
32	1	103	10.15(10)	0.98	54	16	103	11.85(28)	9.40(12)	0.80	11.91(05)	12.40(05)	2.23(03)	aliquot a
32	1	102	10.36(10)	1.03	57	19	102	11.44(23)	9.89(11)	0.94	12.10(06)	12.57(06)	--	aliquot b
32	1	101	9.97(10)	1.03	59	15	101	12.43(37)	9.24(11)	0.82	11.93(05)	12.46(04)	--	aliquot c
32	2	103	10.68(11)	1.15	31	25	103	11.96(16)	9.69(12)	0.87	12.06(06)	12.46(06)	1.97(06)	aliquot a
32	2	106	10.46(10)	1.00	55	17	106	12.40(26)	9.68(11)	0.75	12.15(05)	12.61(04)	2.06(06)	aliquot b
32	2	102	10.44(10)	1.00	53	18	102	12.06(23)	9.66(11)	0.78	12.09(05)	12.55(05)	1.90(04)	aliquot c
32	3	117	10.55(11)	1.14	57	19	116	12.40(23)	9.90(10)	0.87	12.27(06)	12.74(05)	--	
32	4	100	10.48(14)	1.35	42	20	100	10.72(14)	10.20(15)	1.34	11.78(11)	12.16(12)	--	
34	1	100	11.34(11)	1.13	57	18	100	13.93(28)	10.40(10)	0.73	12.81(06)	13.20(05)	2.60(04)	
35	1	101	9.72(11)	1.93	53	19	93	12.25(24)	9.07(12)	0.94	11.88(06)	12.35(06)	1.86(05)	
37	1	50	10.02(12)	0.87	54	20	50	10.93(30)	9.56(16)	0.79	11.79(09)	12.28(09)	--	
38	1	100	9.89(18)	1.76	52	23	94	11.13(18)	9.61(12)	1.12	11.85(08)	12.30(08)	--	
39	1	80	10.99(09)	0.85	--	--	--	--	--	--	--	--	--	

39	2	50	10.32(14)	1.25	--	--	--	--	--	--	--	--	--	
41	1	101	10.34(12)	1.23	--	--	--	--	--	--	--	--	--	
41	2	105	10.31(10)	1.02	--	--	--	--	--	--	--	--	1.82(03)	
41	3	100	9.91(13)	1.26	59	14	98	12.63(52)	9.30(12)	0.83	11.98(05)	12.51(04)	1.42(02)	
41	4	100	10.41(11)	1.05	51	18	98	10.76(19)	10.31(14)	0.86	12.01(08)	12.45(08)	1.80(02)	
41	5	100	10.25(12)	1.17	56	16	99	12.25(32)	9.53(12)	0.95	12.07(06)	12.56(06)	--	Cf
41	6	101	10.09(09)	0.89	59	11	100	12.60(55)	9.47(13)	0.66	12.03(04)	12.54(04)	--	
43	1	96	10.68(10)	1.00	--	--	--	--	--	--	--	--	--	
43	2	95	11.02(14)	1.33	--	--	--	--	--	--	--	--	--	
45	1	100	10.89(10)	1.00	--	--	--	--	--	--	--	--	2.44(07)	
47	1	100	10.29(14)	1.39	53	20	100	13.01(25)	9.09(10)	0.92	12.05(06)	12.52(05)	--	
47	2	100	10.18(14)	1.36	53	20	100	12.87(25)	8.97(10)	0.88	11.97(06)	12.44(05)	--	
47	3	111	9.18(19)	1.99	57	18	96	12.08(28)	8.88(11)	0.90	11.64(06)	12.17(05)	--	